Alma Mater Studiorum · Università di Bologna

Scuola di Scienze
Dipartimento di Fisica e Astronomia
Corso di Laurea in Fisica

Organic small molecules semiconductors as direct X-ray detectors

Relatore:
Prof.ssa Beatrice Fraboni

Correlatore:
Dott.ssa Ilaria Fratelli

Presentata da:
Fabio Raspanti

Anno Accademico 2016/2017

Abstract

Organic small molecules semiconductors are promising in the field of direct ionizing radiation detection.

Unlike their inorganic counterpart, these molecules are easy to work with, since they are flexible, soluble and can be deposited on electronic devices with very simple processes, such as drop-casting and spin-casting. Moreover, these materials have good detection properties and very low working voltage.

To this day, organic semiconductors have mainly been used in indirect radiation detection, employed both in scintillator and as photodetectors. However, direct detection of ionizing radiation is a far more effective method, since it is performed within a single material and a single conversion, directly from photons to electrical signal; furthermore, it provides a higher signal-to-noise ratio and a faster response time.

In this experimental work, I fabricated four direct detectors based on transistors; two different organic solutions were drop-casted onto the transistors, creating a conduction channel between source and drain electrodes.

Both these solutions had chlorobenzene as a solvent, with DiF-TES-ADT and DiF-TEG-ADT as solutes, respectively, in a 0.5% concentration.

The purpose of this thesis is dual. Firstly, I want to study how the detectors' sensitivity is influenced by semiconductor molecules with different Z-number; secondly, I want to test a new drop-casting method (SAC method) and compare it to results previously obtained with traditional deposition methods.

The results are very promising, with very high values of sensitivity obtained with low voltages.

Sommario

I semiconduttori organici a piccola struttura molecolare sono, al giorno d'oggi, molto promettenti nel campo dei rivelatori diretti di radiazioni ionizzanti.

Diversamente dalla loro controparte inorganica, queste molecole sono facilmente utilizzabili in molte applicazioni, grazie alla loro flessibilità, solubilità e alla possibilità di depositarli su componenti elettroniche con processi molto semplici, come il drop-casting e lo spin-casting. Inoltre, questi materiali hanno buone capacità di rivelazione e lavorano con una tensione molto bassa.

Finora, i semiconduttori organici sono stati principalmente utilizzati nella rivelazione indiretta di radiazioni come scintillatori o fotorivelatori. Tuttavia, la rivelazione diretta delle radiazioni ionizzanti è un metodo assai più efficace, perché viene eseguita in un singolo materiale e in un'unica conversione, da fotoni a segnale elettrico. Per questo motivo, fornisce un rapporto segnale-rumore più alto e un tempo di risposta più rapido.

Durante questo esperimento, ho fabbricato quattro rivelatori diretti di radiazioni depositando su dei transistor due diverse soluzioni organiche per drop-casting, creando in questo modo un canale di conduzione fra gli elettrodi di source e drain.

In entrambe le soluzioni è stato usato clorobenzene come solvente, con rispettivamente DiF-TES-ADT e DiF-TEG-ADT come solute in concentrazione 0.5%.

Lo scopo di questo lavoro di tesi è duplice. Il primo obiettivo è studiare come semiconduttori con diverso Z influenzano la sensitivity del rivelatore; il secondo è provare un nuovo metodo di deposizione per drop-casting, chiamato metodo SAC, e confrontarlo con risultati ottenuti in precedenza con metodi di deposizione tradizionali.

I risultati sono molto promettenti, con valori di sensitivity molto elevati ottenuti con un potenziale relativamente basso.

Contents

1. Introduction 3
2. Organic Semiconductors as Radiation Detectors – State of the Art 5
   - 2.1 Radiation sources 5
     - 2.1.1 Radioactivity 5
     - 2.1.2 Sources of radiation 6
     - 2.1.3 Photons 7
     - 2.1.4 Sources of photons – X-ray machines 8
   - 2.2 Organic materials 11
     - 2.2.1 Properties 11
     - 2.2.2 Organic compounds 11
   - 2.3 Organic semiconductors 13
     - 2.3.1 General properties 14
   - 2.4 Organic Thin-film Transistors 15
     - 2.4.1 Properties and operating principles 15
     - 2.4.2 Design and fabrication 19
     - 2.4.3 Applications 21
   - 2.5 Solid-state Organic Molecules Detectors 21
     - 2.5.1 Semiconductors and recombination 21
     - 2.5.2 Drift of electrons and holes 23
     - 2.5.3 Desired properties 23
   - 2.6 Semiconductors' Applications in Indirect Detectors 24
     - 2.6.1 Organic scintillators 24
     - 2.6.2 Photodetectors 27
   - 2.7 Damaging Effects of Radiations on Semiconductors 29
3. Materials and Methods 33
   - 3.1 Detectors' Structure 33
   - 3.2 Sample Fabrication Process 34
     - 3.2.1 Solutions' composition 34
     - 3.2.2 Solutions' deposition method 35
   - 3.3 Electrical Characterization 36
   - 3.4 X-ray Characterization 38
     - 3.4.1 X-ray exposure 39
     - 3.4.2 X-ray effects analysis 40
     - 3.4.3 Data analysis parameters 40
4. Results 41
   - 4.1 Samples 41
   - 4.2 Electrical Characterization 41
     - 4.2.1 Samples TES_S1-TES_S2 42
     - 4.2.2 Samples TEG_S3-TEG_S4 44

4.3 X-ray Characterization 46
4.3.1 Samples TES_S1-TES_S2 46
4.3.2 Samples TEG_S3-TEG_S4 49
4.3.3 Damaging X-ray effects 49
5. Conclusions 51
References 53

1 - Introduction

The detection of ionizing radiations, such as Gamma rays, X-rays, high-energy electrons and Alfa particles, is a growing research area offering development opportunities in many fields, from particle physics to medical analysis.

High-energy photons, which constitute X and Gamma rays, can be detected in two different ways, directly or indirectly.

In both methods, interactions with high-energy photons cause primary excitations and ionizations, which consists in generating electron-hole pairs; these pairs interact then within the detection material and produce more electron-hole pairs (second excitation).

In indirect detection, the electron-hole pairs transfer their energy to a scintillator; the scintillator then releases this energy by emitting radiation, usually in the visible wavelength range. The radiation is successively collected by a photo-multiplier tube or a photodiode and converted into an electrical signal representing the incident radiation's intensity.

In direct detection, an electric field is applied to separate excitons (electron-hole pairs); electrons and holes are attracted to the positive and negative electrodes, respectively, and the resulting photocurrent is associated to the radiation beam.

The main advantage of the latter method over the former is the number of conversions needed. In indirect detection, we have first a conversion from X-rays to visible wavelengths, then another conversion from visible light to electrical signal; in direct detection, on the other hand, we only have one step from photons to electrical signal.

Between the two, direct detection of ionizing radiation is a far more effective method, since it is performed within a single material and provides a higher signal-to-noise ratio and a faster response time.

The properties needed for materials involved in the production of the two types of detectors are similar: high radiation stopping power, in order to have maximum absorption of the incident radiation, good material purity to avoid excitons' trapping and uniformity to reduce radiation scattering.

Organic semiconductors are becoming more and more popular in radiation detection, because of their good detection properties, flexibility and very low working voltage.

To this day, organic semiconductors have mainly been used as scintillators or as photodiodes; in recent years, the research in the field of direct radiation detection made many steps forward, revealing new application opportunities.

The purpose of this study is to further develop our knowledge about the application of these materials as direct ionizing radiation detectors. In particular, I establish two distinct goals.

I study how the detectors' sensitivity is influenced by semiconductor molecules with different Z-number; I chose a silicon-based molecule (DiF-TES-ADT) and a germanium-based one (DiF-TEG-ADT).

Furthermore, different deposition methods for the organic molecules might have different effects on the crystals' structure, which consequently affect the electrical and X-ray exposure properties; therefore, I also analyse how a new drop-casting technique affects the devices' sensitivity. I then compare these results with different deposition methods previously executed (regular drop-casting and spin-casting).

To do so, I create two solutions based on two different organic semiconductors; both the solutions are then applied by means of SAC drop-casting onto the transistors.

Successively, the devices are exposed to ionizing radiations of the X-ray wavelength. Exposition is performed in a dynamic way, with alternating exposure and dark periods, and with different dose rates, in order to get an accurate estimate of the devices' sensitivity.

This work is arranged as follows.

In chapter 2, I examine the current state of the art of organic semiconductors as radiation detectors. I first give a general description of radiation sources and properties of photons. Successively, I briefly show the main features of organic semiconductors and how they are employed in radiation detection; I also discuss the damaging phenomena occurring when these materials are exposed to radiation.

In chapter 3, I present the methods and materials used in this study. I go over the detectors' structure and how they are fabricated; I also describe how electrical and X-ray exposure characterizations are performed.

In chapter 4, I report the obtained results. I first present the electrical characterization results; then, I present the X-ray exposure data and the damaging effects on the detectors.

In chapter 5, I draw conclusions on the results and working methods.

2 – Organic Semiconductors as Radiation Detectors – State of the Art

The research interest on alternative materials for innovative ionizing radiation detection is rapidly growing. Traditional materials for direct, solid-state detectors such as silicon, cadmium, zinc, telluride or mercury iodide, suffer from severe limitations in their processing into large-area pixelated detector matrices.
Therefore, a new type of ionizing radiation detectors needs to be designed, ideally combining ease of processing, low power supply and mechanical flexibility.
In fact, several applications require thin, conformable sensor panels, for a large-area determination of the incoming radiation dose and energy distribution.
As such applications are of high commercial interest, intense efforts have been recently devoted to the realization of large-area direct detectors based on inorganic; these materials, however, still share the limits of expensive or complex growth techniques and maintain stiff mechanical properties.
An alternative, promising approach is based on organic materials as active photodetectors.
One of the interesting features of organic materials is their easy deposition over large areas by solution-coating, which can be done with inexpensive techniques, such as drop-casting, inkjet printing and solution shearing, potentially onto flexible substrates.
Moreover, the typical density of organic molecules is very similar to that of human tissue, making them very interesting for medical X-ray direct dosimetry. [1]

2.1 Radiation Sources

Radiations can be categorized in different ways, such as ionizing and non-ionizing, particles and waves, hazardous and non-hazardous.

However, none of these categorizations draws solid boundaries between properties of individual particles comprising the radiation; rather they show the bulk behavior of particle beams. For example, it will not be correct to assert that an electron always ionizes atoms with which it interacts by arguing that it belongs to the category of ionizing particles.

All we can say is that if a large number of electrons interacts with a large number of atoms, the predominant mode of interaction will lead to the ionization of atoms.

Based on this argument, it is safe to say that the categorization of radiation found in the literature on these bases should not be considered to represent individual particles. What this really means is that if we have a very large number of a certain kind of particles, there is a high probability that most of them would behave in the manner characteristic of their categorization.

The theoretical foundations of particle interaction is quantum mechanics, which quantifies the variables related to particle motion, such as momentum, energy and position, in probabilistic terms. The observable is not the particle, as it is in classical mechanics, but its probability density. [2]

2.1.1 Radioactivity

Radioactivity is the process through which nuclei spontaneously emit subatomic particles.

It was discovered by French scientist Antoine Henri Becquerel in 1896; he found out that uranium emitted something invisible that fogged his photographic plates. The term radioactivity was successively suggested by Marie Curie.

Originally, three types of radiation were discovered:

- α-rays (helium nuclei)
- β-rays (electrons)
- γ-rays (photons)

Later on it was found that other particles such as neutrons, protons, positrons and neutrinos are also emitted by some decaying nuclei. The underlying mechanisms responsible for emission of different particles are different.

The process of internal conversion can occur to electrons in any electronic orbit.

Units of Radioactivity

Since the most natural way to measure activity of a material is to see how many disintegrations per unit time it is going through, therefore the units of activity are defined in terms of disintegrations per second. For example, 1 Becquerel corresponds to 1 disintegration per second and 1 Curie is equivalent to 3.7×10^{10} disintegrations per second.

Curie is a much bigger unit than Becquerel is and is therefore more commonly used. However, for most practical sources used in laboratories, Curie is too big; therefore, its subunits of milli-Curie and micro-Curie are more commonly found in literature. The conversion factor between Curie and Becquerel is given below. [2]

$$1\ \text{Bq} = 1\ \text{disintegration/sec}$$
$$1\ \text{Ci} = 3.7 \times 10^{10}\ \text{disintegrations/sec}$$
$$1\ \text{Bq} = 2.703 \times 10^{-11}\ \text{Ci}$$

2.1.2 Sources of radiation

Radiation sources can be divided into two categories: natural and man-made.

Natural sources

There are three types of natural sources of radiation: cosmic, terrestrial, and internal.

- Cosmic Radiation Sources

  The outer space is filled with radiation that comes from a variety of sources such as burning (e.g., our Sun) and exploding (e.g., Supernovae) stars.

  These bodies produce immense amounts of radiation, some of which reach earth.

  On top of these localized sources of radiation, there is also a background radiation of low energy photons; it is known as cosmic microwave background radiation since the photon spectrum peaks in the microwave region of the electromagnetic spectrum.

  Apart from photons, other particles are constantly being produced in outer space. Most of them, however, never reach the earth either due to magnetic deflection or the earth's upper protective atmosphere.

- Terrestrial Radiation Sources

  This type of radiation is present in small quantities all around us and is more or less inescapable. Our surroundings are contaminated with minute quantities of radiation emitting isotopes.

The main sources of terrestrial radiation are uranium and its decay products such as thorium, radium, and radon.

- Internal Radiation Sources

  Our bodies contain some traces of radioactive elements that expose our tissues to continuous low-level radiation. This internal radiation primarily comes from Potassium-40 and Carbon-40 isotopes; its intensity is however minimal.

Man-made sources

Right after the discovery of radiation and realization of its potentials, scientists started working on developing sources that could be used to produce radiation in controlled laboratory environments. These sources are made for specific purposes and generally give off one type of radiation. Common examples of such sources are

- medical x-ray machines
- airport x-ray scanners
- particle accelerators
- lasers

Out of all these sources, the ones used in medical diagnostics and therapy expose the public to the most significant amounts of radiation. [2]

2.1.3 Photons

A photon represents one quantum of electromagnetic energy and is treated as a fundamental particle in the Standard Model of particle physics. In this model, the photon is assumed to have no rest mass. When the photon is traveling in a medium, it slows down due to interaction with the medium and acquires an effective mass. In vacuum, however, it is considered to be massless.

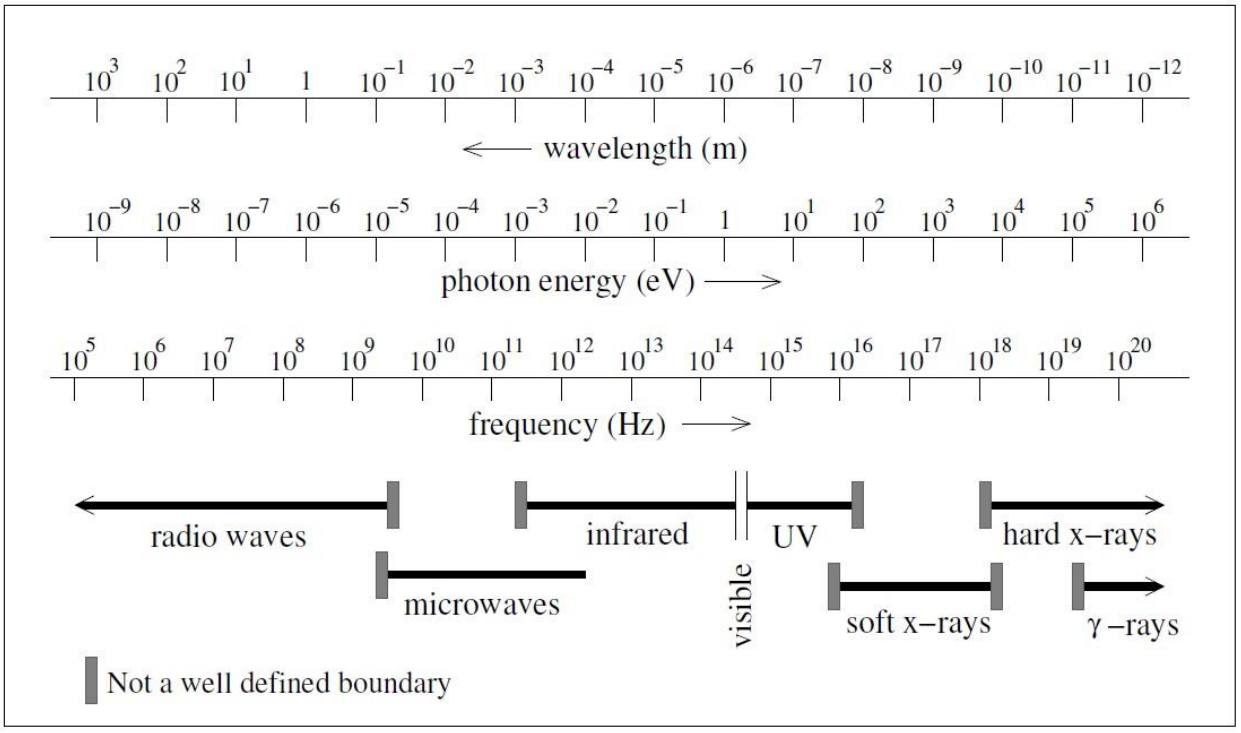

Figure 2.1 - Electromagnetic spectrum [2]

Photons do not correspond to only visible light. In fact, light spans a very narrow region of their full energy spectrum (Figure 2.1).

Photons are involved in all types of electromagnetic interactions.

There are many ways to produce photons that are not in the visible light region of the spectrum. For example, whenever a charged particle moves (such as a changing current in a wire), it creates electromagnetic waves around it that propagate in space. These waves are considered to be excitations in the underlying electromagnetic field and a quantum of these excitations is called a photon.

The energy carried by a photon can be absorbed in a number of ways by other particles with which it interacts. Furthermore, like other particles, a photon can scatter off from other particles and even experience gravitational pull.

In terms of radiation exposure and biological damage, we are generally concerned with high energy photons, such as γ-rays, X-rays, and ultraviolet rays. Having high energies, these photons can penetrate deeper and cause more damage than the low energy photons such as visible light.

An important property of photons is that they carry momentum even though they have no rest mass. The momentum p_γ of a photon with energy E, frequency ν, and wavelength λ is given by: [2]

$$p_\gamma = \frac{E}{c} = \frac{h\,\nu}{c} = \frac{h}{\lambda} \tag{2.1}$$

2.1.4 Sources of photons - X-ray machines

Photons play very important roles not only in physics, but also in engineering, medical diagnostics and treatment.

Since X-rays are high energy photons and can cause considerable damage to tissues, they are produced and employed in controlled laboratory environments. Production of X-rays is a relatively simple process, in which a high-Z target (i.e. an element having large number of protons, such as tungsten or molybdenum) is bombarded by high velocity electrons (Figure 2.2). This results in the production of two types of X-rays: Bremsstrahlung and characteristic X-rays.

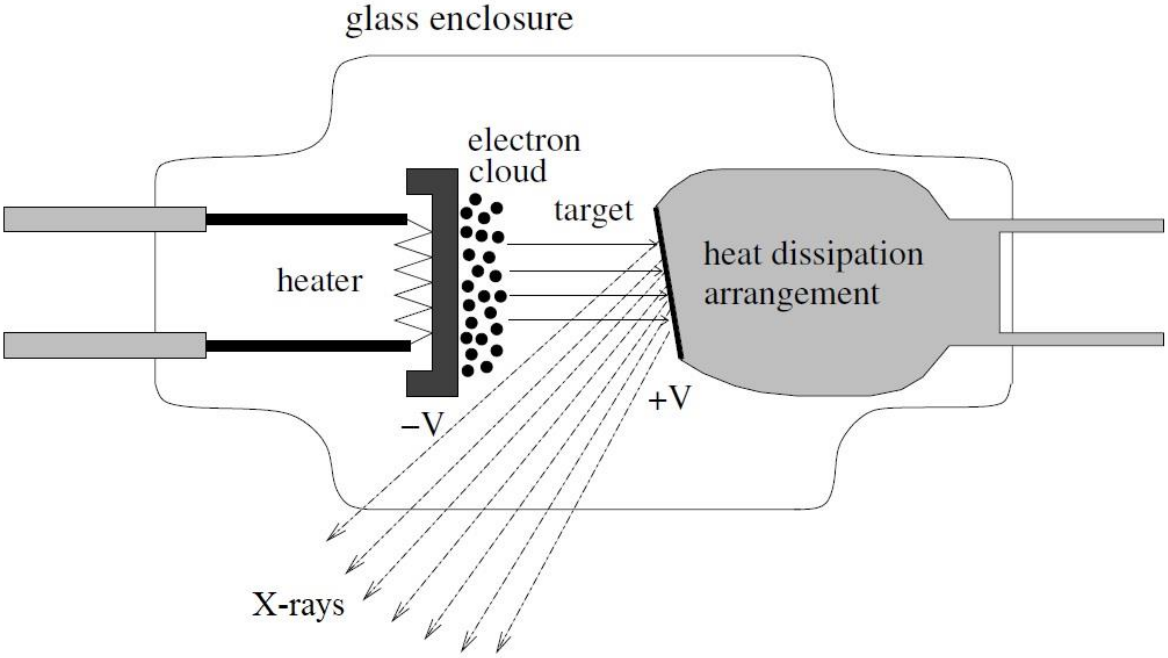

Figure 2.2 - Sketch of a typical X-ray tube [2]

Bremsstrahlung refers to the radiation emitted by charged particles when they decelerate in a medium (Figure 2.2). In case of x-rays, the high-energy electrons decelerate quickly in the target material and hence emit Bremsstrahlung. The emitted X-ray photons have continuous energy spectrum (Figure 2.4), since there are no quantized energy transitions involved in this process.

The electrons incident on the target may also attain sufficient energies to knock off electrons from the internal atomic shells of the target atoms leaving them in unstable states. To regain atomic stability, the electrons from higher energy levels quickly fill these gaps. Since the energy of these electrons is higher than the energy needed to stay in the new orbits, the excess energy is emitted in the form of X-ray photons (Figure 2.3).

The energy of characteristic X-rays does not depend on the intensity of the incident electron beam, because the emitted photons always have the energy corresponding to the difference between atomic energy levels.

Since different elements may have different atomic energy levels, the energy of the emitted characteristic X-ray photons can be accurately predicted.

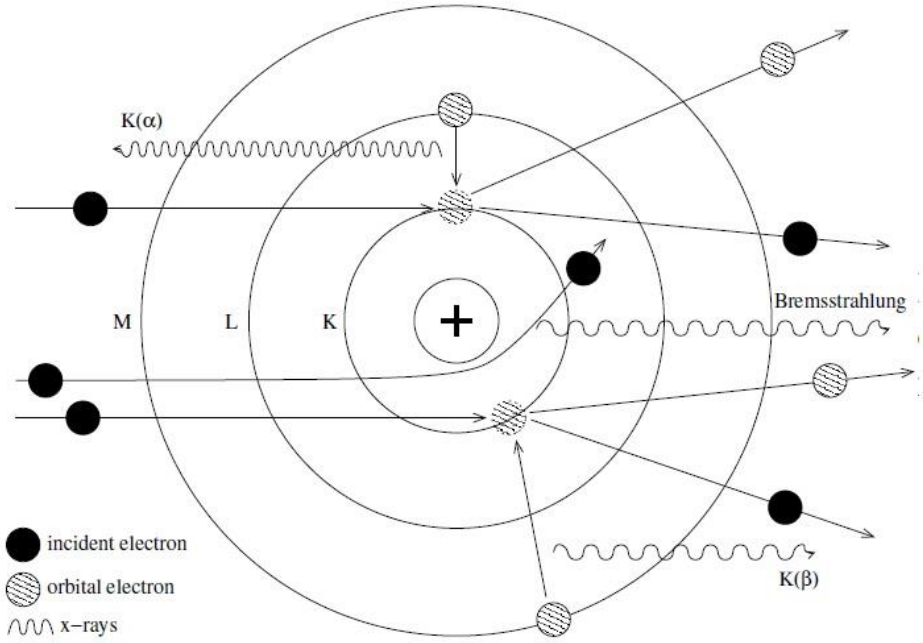

Figure 2.3 - Physical process of generation of characteristic X-rays and Bremsstrahlung [2]

X-ray tube spectra generally have more than one characteristic X-ray peak, since there are a number of electronic transitions possible following a vacancy created in one of the inner electronic shells. If an electron from the innermost K-shell is knocked-off, the vacancy can be filled by any of the electrons in the outer shells. If an electron from the L-shell jumps in to fill the vacancy, a photon with an energy of $E_\gamma = E_L - E_K$ is emitted. A large number of such photons would appear as a prominent peak in the spectrum. Such a peak is generally referred to as K_α peak. K_β peak is the result of transitions of M-shell electrons to the K-shell giving off photons with an energy of $E_\gamma = E_M - E_K$ (Figure 2.3).

In an X-ray tube the target (anode) is kept very close (typically 1-3 cm) to the source of electrons (cathode). A high electric potential between cathode and anode accelerates the electrons to high velocities.

The maximum kinetic energy in electron volts attained by these electrons is equal to the electric potential applied between the two electrodes. [2]

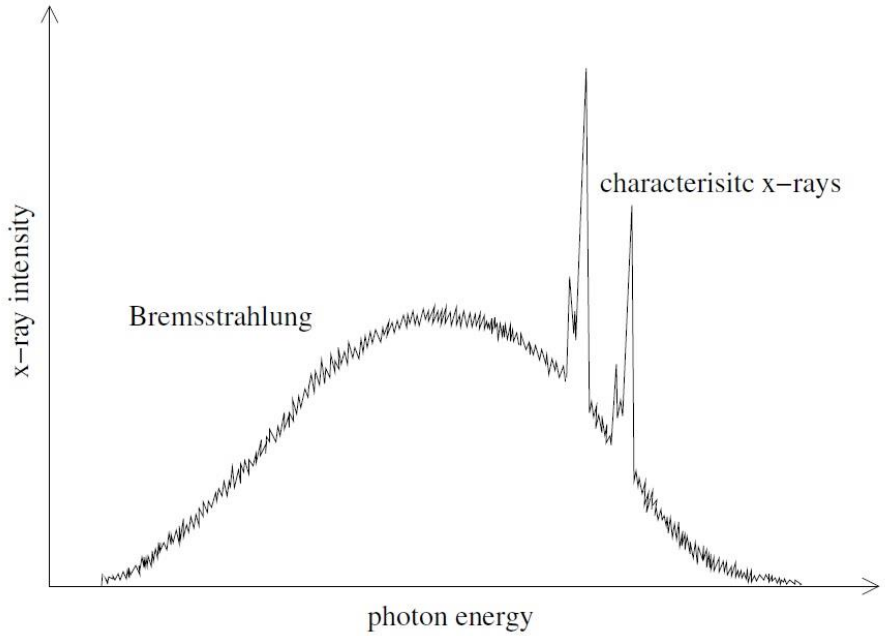

Figure 2.4 - A typical X-ray tube spectrum showing Bremsstrahlung continuum and peaks corresponding to characteristic X-rays [2]

2.2 Organic Materials

Organic molecules are bonded groups of organic elements. The range of chemicals studied in organic chemistry include hydrocarbons (compounds containing only carbon and hydrogen), as well as myriad compositions based always on carbon, but also containing other elements, especially oxygen, nitrogen, sulfur, phosphorus.

In the modern era, the range of organic elements includes:

- Group 1 and group 2 organometallic compounds, i.e., involving alkali (e.g., lithium, sodium, and potassium) alkaline earth metals
- Groups 13-18 of the periodic table, including metalloids such as silicon and germanium. [3][4][5]

2.2.1 Properties

Physical properties of organic compounds typically of interest include both quantitative features, such as melting and boiling points, and qualitative features, like solubility.

Melting and boiling properties

Organic compounds typically melt and many boil. In contrast, while inorganic materials generally can be melted, many do not boil, tending instead to degrade. In earlier times, the melting point and boiling point provided crucial information on the purity and identity of organic compounds. The melting and boiling points correlate with the polarity of the molecules and their molecular weight. Some organic compounds, especially symmetrical ones, sublime, that is they evaporate without melting. A well-known example of a sublimable organic compound is para-dichlorobenzene, the odiferous constituent of modern mothballs. Organic compounds are usually not very stable at temperatures above 300 °C, although some exceptions exist.

Solubility

Neutral organic compounds tend to be hydrophobic, meaning that they are less soluble in water than in organic solvents. Organic compounds tend to dissolve in organic solvents. Solvents can be of various types, such as pure substances like ether or ethyl alcohol, or mixtures, or the range of pure or mixed aromatic solvents such as benzene and its derivatives. Solubility in the different solvents depends upon the solvent type.

Solid-state properties

Various specialized properties of molecular crystals and organic polymers with conjugated systems are of interest depending on applications, e.g. thermo-mechanical and electro-mechanical such as piezoelectricity, electrical conductivity, and electro-optical properties. For historical reasons, such properties are mainly the subjects of the areas of polymer science and materials science. [3][4][5][6][7][8]

2.2.2 Organic compounds

Conjugated cyclic compounds

In chemistry, a conjugated system is a system of connected p-orbitals with delocalized electrons in molecules which are conventionally represented as having alternating single and multiple bonds, which in general may lower the overall energy of the molecule and increase stability.

Conjugation is the overlap of one p-orbital with another across an intervening σ bond.

A conjugated system has a region of overlapping p-orbitals, bridging the interposed single bonds. They allow a delocalization of π electrons across all the adjacent aligned p-orbitals. The π electrons do not belong to a single bond or atom, but rather to a group of atoms.

The largest conjugated systems are found in graphene, graphite, conductive polymers, and carbon nanotubes.Cyclic compounds can be partly or completely conjugated. Annulenes, completely conjugated monocyclic hydrocarbons, may be aromatic, non-aromatic or anti-aromatic.

Aromatic compounds

The term aromaticity is used to describe a cyclic, planar molecule with a ring of resonance bonds that exhibits more stability than other geometric or connective arrangements with the same set of atoms. Aromatic molecules are very stable, and do not break apart easily to react with other substances. Organic compounds that are not aromatic are classified as aliphatic compounds—they might be cyclic, but only aromatic rings have special stability.

Since the most common aromatic compounds are derivatives of benzene, the word "aromatic" occasionally refers informally to this category, and so it was first defined.

Conjugated, planar, cyclic compounds are aromatic and exhibit an unusual stability.

The classic example, benzene, has a system of six π-electrons, which forms the benzene ring along the planar σ-ring with its 12 electrons (Figure 2.5). σ-bonds constitute the molecule's structure, while π-bonds determine the material's electrical properties, since π-electrons are delocalized and they are therefore involved in electrical conduction.

For benzene, there are two equivalent conjugated Lewis structures, so that the true molecular state is a quantum-mechanical combination of the two structures with six equivalent CC

bonds, which are intermediate between single and double bonds, and all of equal length and strength.

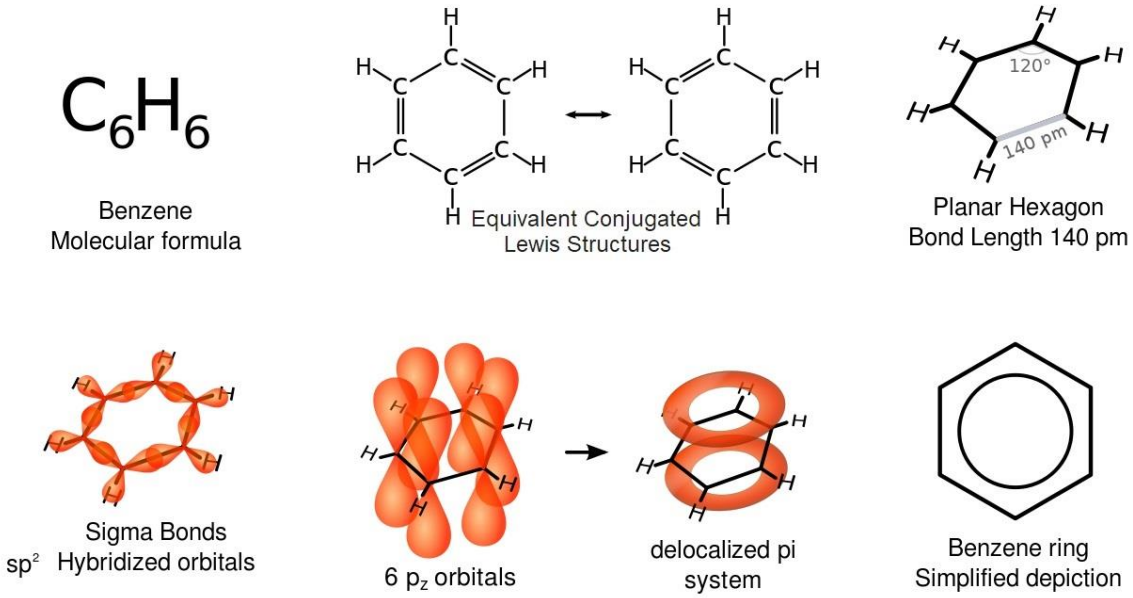

Figure 2.5 – Benzene's structure [6]

Acenes

The acenes or polyacenes are a class of organic compounds and polycyclic aromatic hydrocarbons made up of linearly fused benzene rings. The larger representatives have potential interest in optoelectronic applications and are actively researched in chemistry and electrical engineering. One of the more studied acenes is pentacene, which is often incorporated into organic field-effect transistors and allows to reach high mobility values. [6][7][8][9]

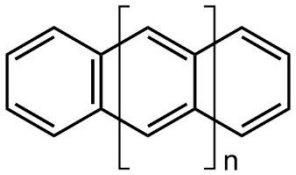

Figure 2.6 – Acenes' structure [6]

2.3 Organic Semiconductors

Semiconductors are crystalline solids in which atoms are held together by covalent bonds. Their name comes from the fact that their electrical conduction properties lie between those of insulators and conductors.

Organic semiconductors are solids whose building blocks are π-bonded molecules or polymers made up by carbon and hydrogen atoms and – at times – heteroatoms such as nitrogen, sulphur and oxygen.

They exist in form of molecular crystals or amorphous thin films. In general, they are electrical insulators but become semiconducting when charges are either injected from appropriate electrodes, upon doping or by photoexcitation. [10]

2.3.1 General properties

In molecular crystals, the energetic separation between the top of the valence band and the bottom of the conduction band, which is commonly referred to as band gap, is typically between 2.5 and 4 eV, while in inorganic semiconductors the band gaps are typically 1 to 2 eV (Figure 2.7).

This implies that they are, in fact, insulators rather than semiconductors in the conventional sense. They become semiconducting only when charge carriers are injected from two electrodes or generated via doping. Charge carriers can also be generated in the course of optical excitation. It is important to realize, however, that the primary optical excitations are neutral excitons. Efficient photogeneration can only occur in binary systems due to charge transfer between donor and acceptor.

In organic semiconductors, orbitals close to the Fermi level are known as HOMO (Highest Occupied Molecular Orbital, the highest orbital in the valence band) and LUMO (Lower Unoccupied Molecular Orbital, the lowest conduction band orbital).

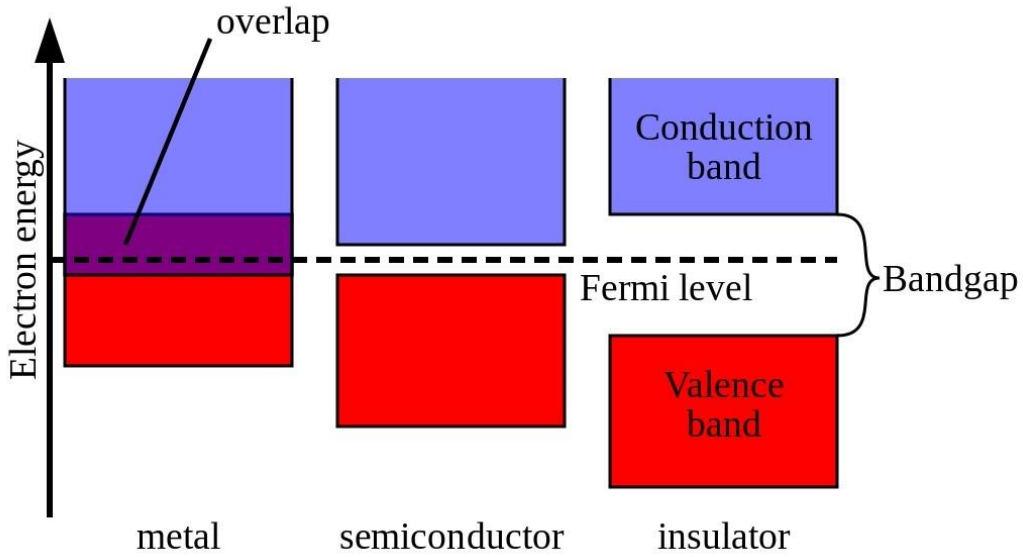

Figure 2.7 – Electron bands in metals, semiconductors and insulators [11]

Otherwise, neutral excitons decay radiatively to the ground state - thereby emitting photoluminescence – or non-radiatively. The optical absorption edge of organic semiconductors is typically 1.7 – 3 eV, equivalent to a spectral range from 700 to 400 nm, which corresponds with the visible wavelength spectrum.

Because small molecule, crystalline organic semiconductors can have high charge carrier mobility (over 40 $cm^2/V \cdot s$) and offer versatile processing possibilities, they can be advantageous for many industrial applications. [10][11]

2.4 Organic Thin-film Transistor

Since John Bardeen, William Shockley, and Walter Brattain invented the world's first transistor in 1947, inorganic field-effect transistors (FETs) have dominated the mainstream microelectronics industry. They are the fundamental building blocks for basic analytical circuits, such as amplifiers, as well as the key elements for digital combinational logic circuits, such as adders, shifters, inverters, and arithmetic logic units, and are used to build sequential logic circuits, such as flip-flops. Moreover, transistors are essential to the modern memory devices, integrated circuits, and microprocessors used in personal computers and laptops.

Organic thin film field-effect transistors (OTFTs) are particularly interesting as their fabrication processes are much less complex compared with conventional Si technology, which involves high-temperature and high-vacuum deposition processes and sophisticated photolithographic patterning methods. In general, low-temperature deposition and solution processing can replace the more complicated processes involved in conventional Si technology. In addition, the mechanical flexibility of organic materials makes them naturally compatible with plastic substrates for lightweight and foldable products.

Although OTFTs are not meant to replace conventional inorganic TFTs – because of the upper limit of their switching speed – they have great potential for a wide variety of applications, especially for new products that rely on their unique characteristics, such as electronic newspapers, inexpensive smart tags for inventory control, and large-area flexible displays.

In this section, I will describe the basic working principle of OTFTs and discuss materials requirements and fabrication methods for building these devices, with the related technical issues and challenges. [12][13]

2.4.1 Properties and operating principles

An OTFT is analogous to its corresponding inorganic device in basic design and function.

It is a three-terminal device in which a voltage applied to a gate electrode controls current flow between a source and drain electrode under an imposed bias (Figure 2.8).

The control of source-drain current in FETs via a third terminal has resulted in their widespread use as switches.

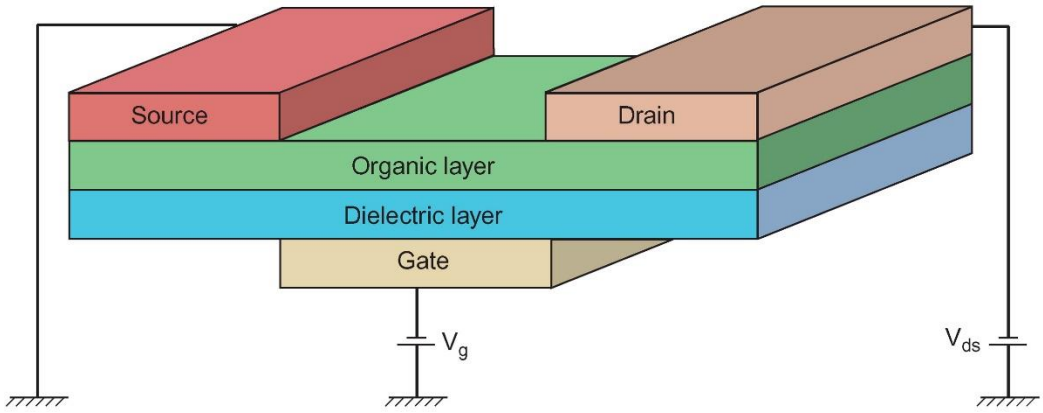

Figure 2.8 - Basic schematic of an organic field-effect transistor [13]

The ideal operation of an n-type OTFT depends on the existence of an electron accumulation layer at the dielectric/semiconductor interface. This ideal operation can be described by analyzing the energy band diagram of the capacitor comprised by the gate electrode, dielectric and semiconductor.

In Figure 2.9, the ideal operation of a n-type TFT is shown: applying a V_G <0 V causes a depletion region at the dielectric interface, while V_G >0 V makes a downward band-bending and the appearance of an accumulation region.

In a real device, the two possible regimes of operation are separated by a voltage value, which corresponds to downward band-bending of the semiconductor close to its interface with the dielectric: the threshold voltage (V_{th}). V_{th} deviates from 0 V, being a function of the gate electrode-semiconductor work function difference, the background carrier concentration of the semiconductor (N), the charge density residing within the dielectric and the trap density at the interface and within the semiconductor.

Depending on the sign of V_{th}, two different mode of operation for TFT can be distinguished: enhancement and depletion for positive or negative threshold voltage, respectively (for n-type TFT).

Once defined the threshold voltage, the role of OTFTs as switches is clear.

For $V_G > V_{th}$, provided that a positive drain voltage (V_D) is applied, current flows between the drain and source electrodes (I_D), corresponding to the logical high state of the TFT.

For $V_G < V_{th}$, regardless of the value of V_D, the upward band-bending of the semiconductor close to the interface with the dielectric is verified, resulting in a low I_D that corresponds to the logical low state.

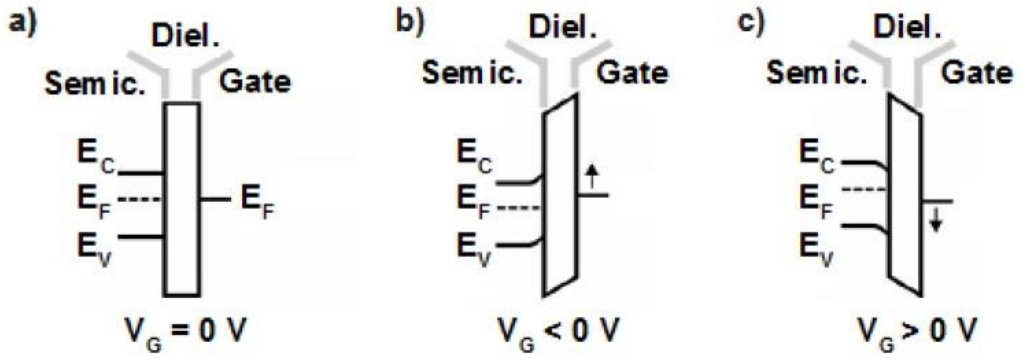

Figure 2.9 - Energy band diagram of an ideal gate electrode/dielectric/n-type semiconductor capacitor for different bias conditions: equilibrium, V_G = 0 V (a); depletion, V_G <0 V (b); accumulation, V_G >0 V(c) [13]

Considering now the logical high state (or on-state) of the OTFT, depending on the intensity of V_D, two different regimes can be distinguished:

1- Pre-pinch off regime $V_D < (V_G - V_{th})$

In this regime the drain current (I_D) can be expressed using the following equation:

$$I_D = C_i \, \mu_{FE} \frac{W}{L} \left[(V_G - V_{th}) V_D - \frac{1}{2} V_D^2 \right] \qquad (2.2)$$

where C_i indicates the capacitance of the dielectric per unit area, μ_{FE} is the field effect mobility and W (width),L (length) are the geometrical dimensions of the channel.

In this regime, a uniform distribution of charge throughout the entire channel is supposed. When a very little voltage is applied through the drain electrode, the second order term in (2.2) can be ignored and the relation between current and voltage drain becomes linear.

2- Post-pinch off or saturation regime $V_D > (V_G - V_{th})$
When the drain voltage overcomes $(V_G - V_{th})$, the accumulation layer close to the drain region becomes depleted, leading to the saturation of I_D.
In the saturation regime the drain current can be expressed by:

$$I_D = C_i \, \mu_{SAT} \frac{W}{2L} [V_G - V_{th}]^2 \qquad (2.3)$$

where μ_{SAT} is the saturation mobility.

Equations 2.2 and 2.3 are based on some assumptions.
The first one was proposed by Shockley and is known as *gradual channel approximation*: the gradient of the lateral field within the channel is negligible compared with the variation of the vertical field. This assumption is not valid near the drain electrode or for short-channel devices in the saturation regime.
Another important assumption is the independence of μ_{FE} and μ_{SAT} from V_G.
The electrical performances of OTFTs are described by several parameters evaluable from the electrical characterization of the devices. In Figure 2.10, the transfer and output characteristic are shown.

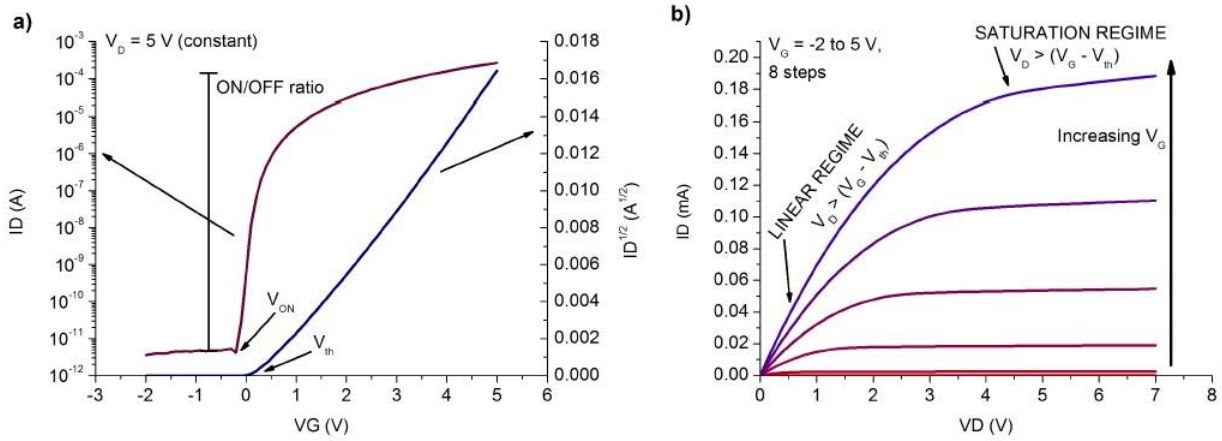

Figure 2.10 - Transfer (a) and output (b) characteristics of an n-type TFT [13]

From these plots, one can extract several parameters like:

On/off ratio
This parameter defines the ratio between the maximum and the minimum value of the drain current. A large value is desirable to obtain a good device for successful usage as electronic switch.

V_{th} / V_{ON}

V_{th} indicates the value to overcome from the gate electrode to achieve an accumulation region in the interface between semiconductor and dielectric layer. This value can be evaluated by a linear extrapolation in the I_D-V_G plot (for low V_D) or in the $(I_D)^{1/2}$- V_G one (for high V_D).

V_{ON} indicates the gate voltage value for which the drain current starts to grow, as it is shown in the transfer characteristic in Figure 2.10a.

Subthreshold swing (S)

S is defined as the inverse of the maximum slope of the transfer characteristic. It represents the necessary V_G to increase I_D by one order of magnitude.

$$S = \left(\frac{\partial \log(I_D)}{\partial V_G}\right)^{-1}_{max} \tag{2.4}$$

Mobility μ

Mobility is related to the efficiency of carriers transport in a material and is directly connected to the maximum I_D and to the switching speed of the devices. For instance, it has a direct impact on the maximum operating frequency or cutoff frequency f_{co}, which can be defined as:

$$f_{co} = \frac{\mu V_D}{2\pi L^2} \tag{2.5}$$

The mobility is directly affected by the scattering mechanisms present in the material, for examples by lattice vibrations, ionized impurities, grain boundaries and other structural defects. In the case of TFTs, where the charges have to flow in a narrow region near the dielectric interface, we have to consider other mechanisms of scattering such as Coulomb scattering from dielectric charges and from interface states or surface roughness scattering.

As it has already been said, the mobility is modulated by V_G and for this reason, depending on the regime, several type of mobility can be calculated:

Effective mobility μ_{eff}

Obtained by the conductance ($g_d = \frac{I_D L}{V_G W}$), with low V_D:

$$\mu_{eff} = \frac{g_D}{2\pi L^2} \tag{2.6}$$

This value is difficult to obtain, because it requires the knowledge of V_{th}. Besides, this is very sensitive to contact resistance because of the low V_D.

Field effect mobility μ_{FE}

Obtained with the transconductance ($g_m = \frac{\partial I_D}{\partial V_G}$), with low V_D:

$$\mu_{FE} = \frac{g_m}{C_i \frac{W}{L} V_D} \tag{2.7}$$

This value is easier to obtain because, the transconductance is extractable from the transfer characteristic and it does not require the knowledge of V_{th}. On the other hand, the contact resistance affects this mobility.

Saturation mobility μ_{SAT}

Obtained with high V_D:

$$\mu_{SAT} = \frac{\left(\frac{\partial\sqrt{I_D}}{\partial V_G}\right)^2}{\frac{1}{2}C_i\frac{W}{L}V_D} \tag{2.8}$$

This mobility does not require V_{th} and it is less sensitive to the contact resistance, but it describes a situation where the channel is pinched-off and its effective length is smaller than L. [12][13]

2.4.2 Design and fabrication

As previously mentioned, the OTFT inherits its design architecture from its inorganic counterpart, namely the metal-oxide-semiconductor field-effect transistor (MOSFET). It is composed of three main components: source, drain, and gate electrodes, a dielectric layer and the active semiconductor layer. Within the basic MOSFET design, there are two types of device configuration: top contact and bottom contact. The former involves building source and drain electrodes onto a preformed semiconductor layer, whereas the latter is constructed by depositing the organic over the contacts (Figure 2.11). Top contact devices have been reported to have superior performance for certain organic semiconductors compared with their bottom contact counterparts. It has been suggested that this is a result of reduced contact resistance between the electrode and the organic layer because of an increase in the area for charge injection.

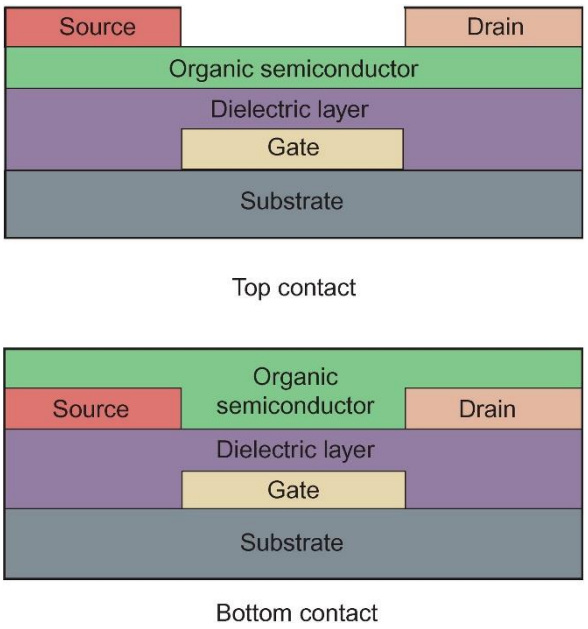

Figure 2.11 - Top and bottom contact OTFT architectures [13]

TFTs are quite similar to other field-effect devices in terms of operation and composing layers, however some important differences exist. While in TFTs the substrate is an insulator, in MOSFETs the silicon wafer plays the role of semiconductor and mechanical substrate at the same time.

Furthermore, fabrication is performed at different temperatures: for MOSFET, a temperature of 1200 K is commonly reached; for TSTs, on the other hand, a lower limit is imposed because of the softening point of the substrate.

MOSFETs have a p-n junction at the source and drain regions, which are absent in the TFTs.

Even if both the transistors' operation is based on field effect, MOSFETs work in inversion regime, while TFTs work in the accumulation one.

In a traditional inorganic device, the active semiconductor layer is generally comprised of lightly doped Si, or combinations of Group III-V elements, such as GaAs. In these materials, the applied gate voltage causes an accumulation of minority charge carriers at the dielectric interface, e.g. electrons in a *p*-type material, termed an 'inversion layer'. In this very shallow channel, carriers injected from the source and drain electrodes may pass, resulting in current flow.

In an organic transistor, on the other hand, the active layer is comprised of a thin film of highly conjugated small molecules or polymers.

In stark contrast to inorganic materials, organics pass current by majority carriers, and an inversion regime does not exist. This fundamental difference is related to the nature of charge transport in each of these semiconductors.

In well-ordered inorganics (e.g., single-crystal Si), the delocalization of electrons over equivalent sites leads to a band-type mode of transport, with charge carriers moving through a continuum of energy levels in the solid.

In less-ordered organic materials, the proposed mechanism is hopping between discrete, localized states of individual molecules. The presence of impurities or inconsistencies in structure may result in "traps" that alter the relative energy levels, and inhibit the flow of charge carriers.

The complexities of current flow in organic materials – which are still not fully understood – have added another dimension to the development of the devices that incorporate them.

In addition to the challenges presented by fabrication, particular attention must be paid to the design of materials that will meet the performance demands of the OTFT in its parent applications. This aspect of development has received much attention, and will continue to play an important role as the technologies progress.

The limitations of current organic technologies are clearly posed by the performance and ease of processing of the active layer component. In addition to meeting benchmarks for performance criteria, such as mobility and on/off ratio, active layer materials should ideally be easy to process, mitigating potential fabrication challenges, and have long-term stability for device longevity. This has proven a difficult balance.

Deposition methods

Deposition of thin film organic semiconductor layers is primarily performed through vapour or solution phase processes. Vacuum deposition is used for small molecules and oligomers. It produces films that show high field-effect mobility and on/off ratios, but it is somewhat costly because of expensive equipment and low deposition throughput.

OTFT device performance can be improved by controlling the deposition rate and temperature, which affect the morphology of the semiconductor. [12][13]

2.4.3 Applications

Organics have long been attractive for use in electronics because of their lightweight, flexibility, and low cost compared with their inorganic counterparts. In addition, recent increases in performance have rapidly expanded the range of possible organic FETs applications, making them targets for a wider range of applications.

Organics offer potential advantages in displays, where TFTs are implemented as switches to activate individual pixels.

Hand-held devices with ultrathin displays can achieve higher resolution and information content, while new technologies, such as flexible displays and electronic paper, get closer to being achievable.

In conclusion, the physical properties and relatively easy processing of organic materials allow for the creation of flexible, low-cost, large-area devices using OTFTs. Advances in fabrication methods and the development of higher-performance semiconductor materials have improved on existing technology and expanded the scope of potentially realizable applications. Much of this progress has been a result of the deduction of the relationship between performance and structure of the active layer component.

Molecular tuning based on this understanding has produced materials with better electronic properties and easier processing. While challenges exist for large-scale manufacturing, the rapid development of these materials shows great promise for their future in plastic electronics. [12][13]

2.5 Solid-state Organic Molecules Detectors

The use of organic materials in ionizing radiation detection is very interesting, thanks to their low cost, flexibility, and simple fabrication compared to the corresponding inorganic materials.

I know describe how semiconductors behave when they are hit by an incident radiation beam, how they can be used to detect radiation and which properties they should have for this purpose.

I will then mention how semiconductors have mainly been used in detectors to this day, i.e. as scintillators and photodetectors. [1]

2.5.1 Semiconductors and recombination

Radiation passing through a semiconductor material is capable of causing the following three phenomena to occur in the bulk of the material:

1- Lattice excitation: the incident radiation deposits energy to the lattice increasing its vibration.
2- Ionization: the incident radiation causes an electron to gain enough energy to break its bond with an atom; an electron-hole pair is produced'
3- Atomic displacement: this non-ionizing phenomenon is the major contributor to the bulk of the damage caused by radiation.

In semiconductor detectors, the main phenomenon is on the ionization process, but lattice excitations also has a significant impact on the electron-hole pair production.

In a perfect semiconductor material, at a temperature below the band gap energy, all the electrons are in valence band. The conduction band in such a situation is completely empty.

The outer shell electrons, taking part in the covalent bonding between lattice atoms, are not free to move around in the material. However, as the temperature raises, some of the electrons could get enough thermal excitation to leave the valence band and jump to the conduction band. This creates an electron deficiency, or a net positive charge, in the valence band and is generally referred to as a *hole*.
This process can also occur, although at a much higher rate, when radiation passes through the material. If a radiation is capable of delivering energy above a material-specific threshold, it is possible to have the creation of electron-hole pairs in the material.

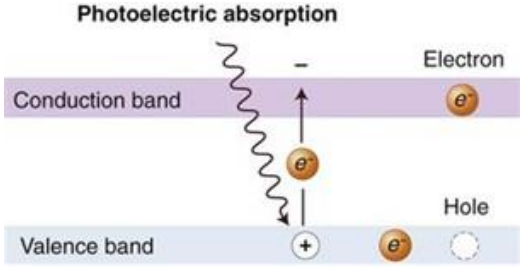

Figure 2.12 – Electron-hole pair production [11]

This threshold is higher than the band gap energy of material, because some of the energy is expended in increase crystal excitations.
For silicon the threshold is very low (3.62 eV), which makes it highly desirable for use in radiation detectors.
In semiconductors, as in gases, the average energy needed to create an electron hole pair is independent of the type of radiation; it depends exclusively on the semiconductor material and its temperature.
The process of ionization in semiconductors is similar to the ionization in gases, but the energy needed in semiconductors is much lower, between 10% and 25%.
This implies that, the radiation being equal, the number of charge carriers produced in a semiconductor is much higher than in gases.
Because of this property, semiconductor detectors are considered to be superior than gaseous detectors.
The free charges in a semiconductor can drift under the influence of an externally applied field. Just like in metallic conductors, their movement can also be characterized by a parameter called conductivity, which quantifies the ability of the material to conduct electric current. However, as opposed to metallic conductors, there are some mechanisms that can contribute to or suppress the conductivity of a semiconductor.
An important factor in semiconductor-based detectors is the quality of the crystal lattice.
If there were imperfections or impurity in the crystal, energy level in the forbidden gap would be produced, causing a degradation in the production of charge pairs. This would cause imperfections and non-linearities in the detector's response through an effect called charge "trapping".
In a trapping process, an electron jumping to an impurity level could be trapped there for some time.
This electron can then do two things: it can either jump up into the conduction band, completing the process of electron-hole pair generation, or fall back into the valence band and recombine with the hole. In the former case, a time delay is introduced in the charge pair production, while in latter no charge pair is produced; the excess energy in this case is not enough to create an electron hole pair, since it will be equal to the energy of the impurity, not to the energy of the gap, and is absorbed by the lattice.

Another process that needs to be taken into account is the band-recombination. In this process, an electron falls from the conduction band into the valence band to recombine with a hole; this form of recombination is the simplest and most prevalent in semiconductors. The result of this process is the removal of the electron from the conduction band and the hole from the valence band. [2]

2.5.2 Drift of electrons and holes

The semiconductor detectors are usually operated in the so-called photoconductive mode; such an operation involves establishment of an electric field across the material.
When the incident radiation produces electron hole pairs along its track in the detector, the charges start moving in opposite directions under the influence of the applied electric field. The velocity with which the charges move depends on the electric field.
For low intensity fields, it has been found that the velocity increases almost linearly with the field strength:

$$\vec{v} = \mu \vec{E} \tag{2.9}$$

where E is the electric field applied and μ is a proportionality constant called mobility. Its value depends on the type of the material.
As the field is further increased, the velocity of the carriers starts showing deviation from the above relation and eventually saturates; most of the detectors are built such that the charges can very quickly attain the saturation velocity, within a few picoseconds.
Based on the drift of electrons and holes, we should now find a proportionality between a measurable quantity and the energy deposited by the incident radiation.
As the charges move in opposite directions, they constitute an electric current with a current density J, which follows Ohm's law:

$$\vec{J} = \sigma \vec{E} \tag{2.10}$$

where σ is the conductivity.
Since current density can also be written as

$$\vec{J} = \rho \vec{v} \tag{2.11}$$

where ρ is the charge density, equations 2.9, 2.10 and 2.11 can be combined to give

$$\sigma = \mu \rho \tag{2.12}$$

If now this material is placed in an ionizing radiation field, electron-hole pairs will be created and consequently the number of free charge pairs in the bulk of the material will increase. The result of this will be a change in the conductivity of the material. If n' represents the number of charge pairs created by the incident radiation, then the change in the conductivity will be given by:

$$\delta\sigma = e \mu n' \tag{2.13}$$

This change in conductivity is proportional to the energy delivered by the incident radiation, provided all other conditions remain constant. Hence measuring the change in conductivity is equivalent to measuring the delivered energy.
Such a measurement can be done by placing the detector in an external circuit, which could measure the change in current caused by change in conductivity.
It should be mentioned here that both electrons and holes take finite amount of time to recombine. Therefore, the output signal actually has a shape with a finite rise and decay times. [2]

2.5.3 Desired properties

The desired properties of semiconductor detectors are highly dependent on the designated application as some of these have conflicting requirements.

Semiconductor detectors are highly versatile devices that can be used both in high and low radiation environments, providing that they are built for specifically for that radiation field. For instance, an avalanche photodiode can be used to detect single photons, but would be useless for detecting high intensity radiations, such as gamma rays.
Therefore, we can divide semiconductor detectors in two categories, depending on whether they are used for high or low radiation fields.
For high radiation environments, the most important properties a detector should have are:

- Charge collection efficiency: with high incident radiation rates, large numbers of charge carriers are generated, so a high collection efficiency is required for the electrodes; electron-hole recombination and charge trapping cause deteriorations in charge collection.
- Fast response: the electronics associated with the detector should be fast enough to distinguish between signals that are a few nanoseconds apart.
- Radiation Hardness: the detector should be as resistant to radiation damage as possible.

For low radiation environments, on the other hand, the requirements are different:

- Charge yield: the number of electron-hole pairs created should be enough to provide a good signal to noise ratio.
- Resolution: high energy resolution is essential in low radiation conditions. [2]

2.6 Semiconductors' Applications in Indirect Detectors

High-energy photons can be detected with two different methods, directly or indirectly.
In both methods, interactions with high-energy photons cause primary excitations and ionizations, which consists in generating electron-hole pairs; these pairs interact then within the detection material and produce more electron-hole pairs (second excitation).
In direct detection, an electric field is applied to separate excitons (electron-hole pairs); electrons and holes are attracted to the positive and negative electrodes, respectively, and the resulting photocurrent is associated to the radiation dose absorbed by the detector.
In indirect detection, the electron-hole pairs transfer their energy to a scintillator; the scintillator then releases this energy by emitting radiation, usually in the visible wavelength range. The radiation is successively collected by a photodetector (a photo-multiplier tube or a photodiode) and converted into an electrical signal representing the incident radiation's intensity.
Indirect detection is less effective, since it causes a lower signal-to-noise ratio and a slower response time. Furthermore, it is performed using multiple devices, resulting in a bulky, inconvenient detector.
To this day, organic semiconductors have mainly been used as scintillators or as photodiodes. In this section, I discuss the main features of scintillators and photodetectors. [14]

2.6.1 Organic scintillators

Organic scintillators are extensively used in radiation detectors. They are found in solid, liquid, and gaseous states. One of the most important advantages of organic scintillators is that they can be produced in virtually any geometry, therefore can be customized to specific applications.

Scintillation Mechanism
The basic scintillation mechanism of organic scintillators is the fluorescence or prompt emission of light following the S-state electronic transitions (Figure 2.13).

The incident radiation transfers energy to the atoms causing electronic transitions from S_0 ground levels to different vibrational levels in the S_1 band; higher band transition are also possible, depending on the energy of the incident radiation.

The induced instability in the system forces the electrons in different S_1 vibrational levels to go to the S_1 ground level through radiation-less transitions.

These transition are very fast, they are completed within a few tenths of a nanosecond. From there the electrons fall into the S_0 ground and vibrational levels with decay times on the order of a few nanoseconds.

The excess energy of the electrons is emitted in the form of fluorescence photons, which for most materials lie in the ultraviolet or visible region of the electromagnetic spectrum.

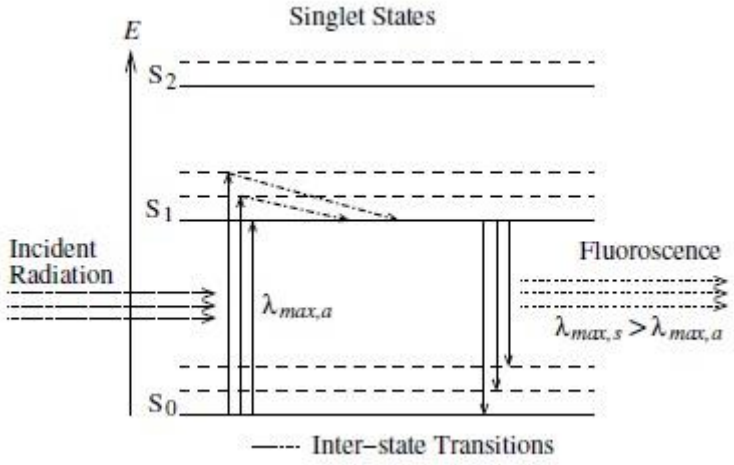

Figure 2.13 - Typical singlet energy level diagram of organic scintillators [2]

The decay of electrons from the S_1 vibrational states to S_1 base level is a favorable process especially for scintillation detectors, because during such decays the electrons loose some of their energy.

Consequently, the energy emitted during their transitions from the S_1 ground level to the S_0 levels is less than the energy absorbed during the radiation-induced transitions from S_0 ground level to S_1 levels. This essentially implies that the absorption and emission spectra of such materials do not match, hence disfavoring the re-absorption of the scintillation light in the material.

This phenomenon was first observed by Sir George G. Stokes, who later on formulated a principle stating that the wavelength of fluorescence light is always greater than the wavelength of absorption. This law does not really hold for all wavelengths and all materials since there is always some overlap of emission and absorption spectra.

However, the so-called *Stoke's shift* is evident, the emission spectrum's peak is shifted from the absorption spectrum's peak.

Stoke's shift between absorption and emission spectra can be defined as:

$$\Delta\lambda_{Stokes} = \lambda_{max,e} - \lambda_{max,a} \tag{2.14}$$

Where λ_{max} represents the peak of the spectrum with subscripts *e* and *s* referring to the emission and absorption, respectively.

A typical emission and absorption spectra of an organic scintillator is represented in Figure 2.14. In general, the higher the Stoke's shift, the smaller the probability of re-absorption of scintillation light since the overlap area will be smaller.

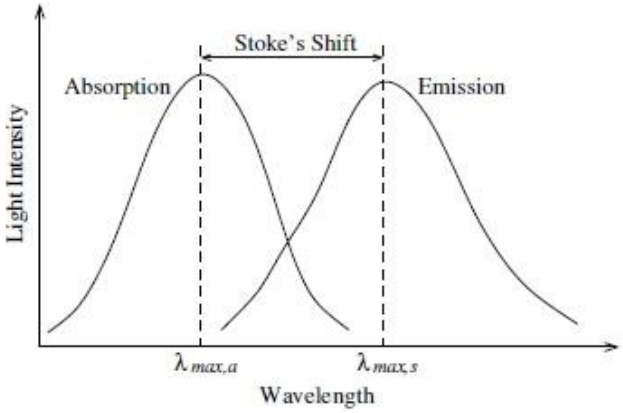

Figure 2.14 - Typical absorption and emission spectra of an organic scintillator [2]

The above-mentioned transitions is not the sole possible in organic scintillators. Another mode of electron relaxation is through the vibrational levels in the triplet T_1 band (Figure 2.15).

As before, the incident radiation transfers the electrons from the S_0 ground level to the S_1 vibrational levels. These electrons first decay into the S_1 ground level through radiation-less transitions. Successively, instead of falling into the S_0 level directly, the electrons can first go to the available T_1 levels.

These triplet levels are much more stable than the singlet levels and consequently the electrons can be thought of being trapped there for an extended time. From the T_1 ground level, into which all electrons eventually decay, they fall into the S_0 levels.

This also results in the emission of light, but in this case it is called phosphorescence or delayed fluorescence, since it is emitted after a substantial delay, which is more than 100 ms for typical organic scintillators.

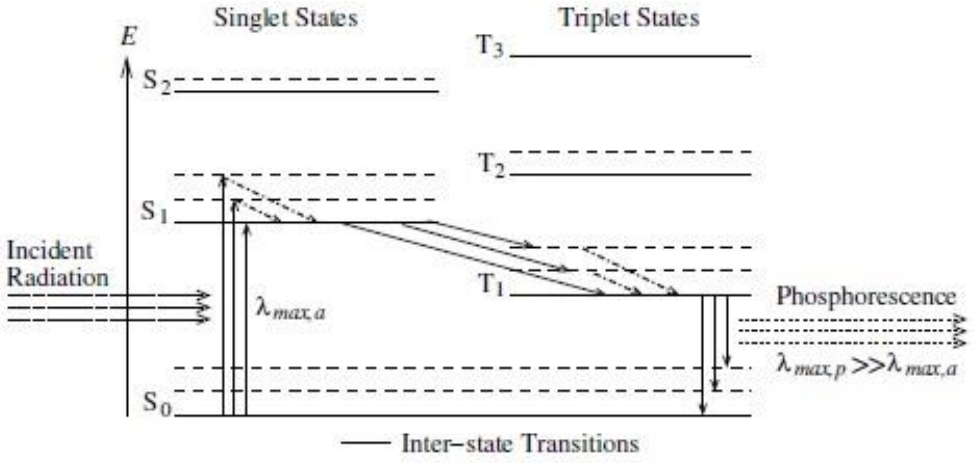

Figure 2.15 – Alternative energy level diagram of organic scintillators. [2]

Transfer of scintillation photons

Scintillators produce photons of certain wavelengths that normally fall within the visible region of the electromagnetic spectrum.

To detect these photons, photodetectors are used. I will now discuss how the scintillation photons are transferred from the scintillator to the photodetector.

The simplest way to do this is to directly attach a scintillator to a photodetector with greater area, in order to avoid losing photons.

However, the geometries of scintillators and photodetectors normally cannot satisfy these characteristics, with the scintillators usually having areas larger than the photodetectors'.

Hence building a detector in such a configuration is generally not possible.

A more practical approach is to use a light guide to connect the photon-emitting surface to the photodetector in such a way that the scintillation photons reach the photodetector with minimal loss.

A light guide can be constructed in different configurations, but all of them are based on the principle of reflection. [2]

2.6.2 Photodetectors

The photons produced by scintillators can be detected in a number of ways, the most notable of which are photomultiplier tubes (PMTs) and photodiodes (PDs).

Both of these detector types have their own pros and cons. For example, photomultiplier tubes have sensitive mechanical structures that are prone to damage in mechanically unstable environments, while the photodiodes are made of semiconductor materials and are therefore mechanically stable.

On the other hand, the response time of PMTs is much smaller than photodiodes, therefore PMTs are preferred in timing applications.

These are only two of the parameters and the choice of a photodetector is in reality a compromise between many factors, including cost.

Photomultiplier tubes

Photomultiplier tubes are sensitive devices that are capable of converting light photons into a very large number of electrons.

The basic building blocks of a complete PMT are a photocathode, an electron multiplication structure, and a readout electrode.

The photons incident on the photocathode are converted into electrons through photoelectric effect. The electrons are then accelerated and strike a metallic structure called dynode, resulting in the emission of more electrons.

The newly produced electrons are again accelerated towards another dynode, where even more electrons are produced. This process of electron multiplication continues until the electrons reach the last dynode, where an ammeter measures the resulting current (Figure 2.16).

The most important characteristics that make PMT-based photodetectors desirable for radiation detection are:

- High sensitivity
- Good signal-to-noise ratio
- Fast time response
- Large photosensitive area.

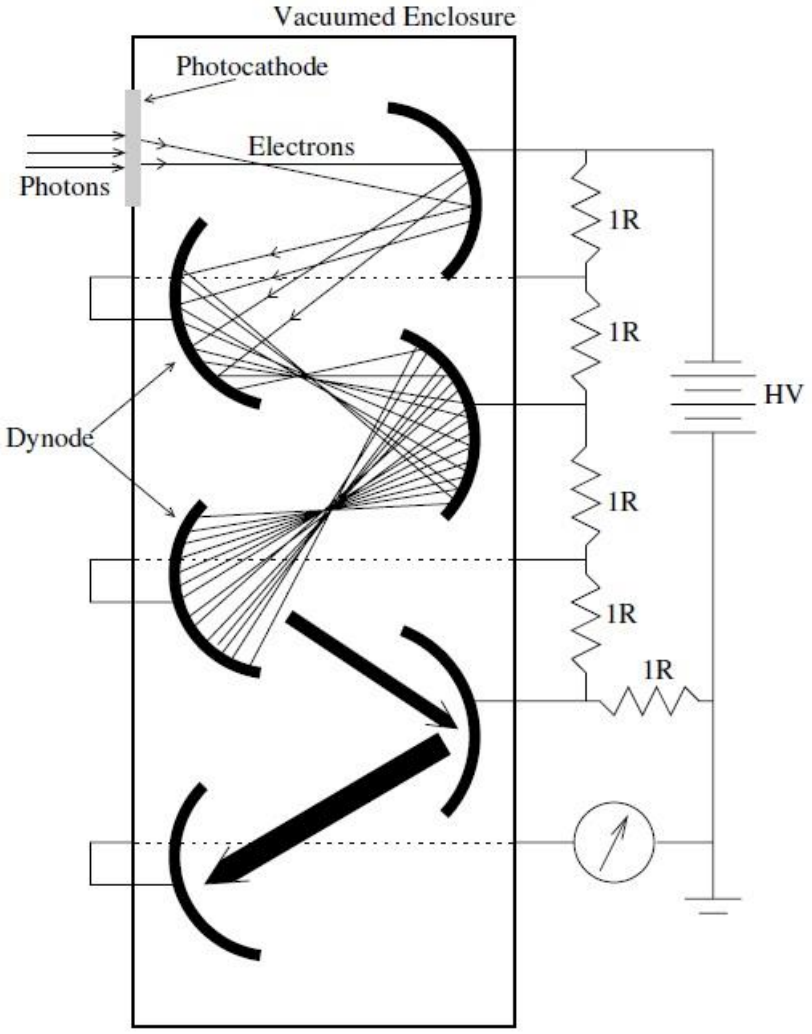

Figure 2.16 – Working principle of a PMT; in real applications, 10 or more dynodes are used. [2]

With rapidly developing technology, new photodiode are now being able to match or even surpass these properties.

Photodiode Detectors

A photodiode is a semiconductor device that converts light into an electrical current. When photons collide with the device, a current is generated by photoelectric effect. Photodiodes may contain optical filters, built-in lenses, and may have large or small surface areas. They usually have a slower response time as their surface area increases. The traditional solar cell used to generate electric solar power is a large area photodiode.

Photodiodes are similar to regular semiconductor diodes, except that they may be either exposed, to detect UV or X-rays, or packaged with a connection to allow light to reach the sensitive part of the device. Many diodes designed for use specifically as a photodiode use a PIN junction rather than a p–n junction, to increase the speed of response. A photodiode is designed to operate in reverse bias.

The material used to make a photodiode is critical to define its properties, because only photons with sufficient energy to excite electrons across the material's bandgap will

produce significant photocurrents. Because of their greater bandgap, silicon-based photodiodes generate less noise than germanium-based photodiodes.

Advantages of photodiodes over photomultipliers include:

- Good linearity of output current as a function of incident light
- High signal-to-noise ratio
- Good endurance to mechanical stress
- Lower cost
- Light weight and small size
- Low operation voltage.

On the other hand, disadvantages compared to photomultipliers include:

- Small area
- No internal gain
- Low overall sensitivity
- Slow response time. [2][15][16][17][18]

2.7 Damaging Effects of Radiations on Semiconductors

A serious problem with semiconductors is their vulnerability to structural damage caused by radiation. Both instantaneous and integrated doses contribute to the overall damage. Although some of these effects can be compensated by increasing the reverse bias, eventually the bulk of the damage renders the detector material useless.

Therefore, deployment of semiconductor-based detectors in highly hostile radiation environments, such as particle accelerators, needs careful consideration and regular monitoring.

Damage Mechanism and NIEL Scaling

The most damaging defects caused by radiation are the result of atomic displacements that destroy the lattice structure. These defects could be dispersed or clustered around the incident radiation track.

Dispersed atomic displacements cause the so-called point defects.

A cluster of such displacements in close vicinity to each other is called cluster defect. The distinguishing feature of clustered defects is that they make a large region of the bulk of the material useless.

The main damage mechanism is the displacement of an atom from its lattice site by an incident particle; this is called Non Ionizing Energy Loss or NIEL.

As opposed to the ionizing energy loss, NIEL is not proportional to the total energy absorbed in the semiconductor and is highly dependent on the type of radiation and its energy.

It should also be mentioned that the atoms displaced by the incident radiation can cause further damage. However, since these recoil atoms usually have a low energy, this effect is not very pronounced.

Hence, in this case NIEL scaling will be a good approximation of the overall damage.

In the case of high energy neutrons, however, the recoil spectrum is more skewed towards the high energy end and therefore NIEL scaling should be interpreted carefully. Independently from which specific damage mechanism is caused, the end result is the performance deterioration of the detector.

Shown below are the most important of these deteriorating effects on the detector performance.

Leakage current

One of the main radiation induced damages is the change in reverse bias current; this phenomenon is caused by the increase or decrease in the number of free charge pairs in the depletion region.

The decrease in leakage current, which is generally observed during initial irradiation, is primarily due to production of charge traps in the forbidden energy gap.

After prolonged irradiation, the leakage current can show significant increase, as the probability of charge pair production increases by introduction of additional energy levels in the forbidden gap.

It has been found that the damage-induced leakage current depends on the radiation dose rate, the exposed volume of the detector, and its temperature.

The dose rate is the amount of absorbed radiation per mass unit and depends of course on the particle flow, which is simply the integrated radiation intensity.

At a certain temperature, the dependence of change in leakage current Δi_l on particle flow Φ and volume V can be written as:

$$\Delta \mathrm{i}_l = \alpha \, \mathrm{V} \, \Phi \tag{2.15}$$

where α is the so-called *damage coefficient* and depends on the type of incident particle and its flow.

This equation can also be written in terms of leakage current before irradiation i_0 and after irradiation i_r:

$$i_r \; = \; i_0 + \alpha \, \mathrm{V} \, \Phi \tag{2.16}$$

The temperature dependence of i_r, on the other hand, can be described by Boltzmann function:

$$i_r(T) \; \propto \; T^2 \, e^{-E/2kT} \tag{2.17}$$

where T is the absolute temperature and k is the Boltzmann's constant; E is the activation energy of the material, which is generally higher for irradiated material.

The change in leakage current has unwanted consequences on detector performance, most notably increase in noise and consequent deterioration of signal to noise ratio.

Fortunately, this strong dependence can be easily exploited to compensate for the deterioration by decreasing the operating temperature.

This is a common practice for detectors used in hostile radiation environments, such as particle accelerators, where radiation induced damage is generally very high.

Type Inversion

A special type of damage caused by high intensity radiation is the inversion of the material's type, in which an n-type material may change into a p-type and vice versa after prolonged irradiation.

This phenomenon can be easily understood by noting that radiation damage has the overall effect of changing the effective dopant concentration in the bulk of the material by increasing the charge carriers of the opposite sign. With increase in radiation dose rate, the original effective dopant concentration may be overcome by the charges of opposite sign.

This effect has been observed specially in silicon detectors in hostile radiation environments. What happens is that the radiation creates acceptor sites, which capture electrons resulting in a decrease in effective doping level. This continues until the donor level becomes equal to the acceptor level, changing the material into intrinsic type.

Further irradiation increases the acceptor level and consequently the types of material changes (Figure 2.17).

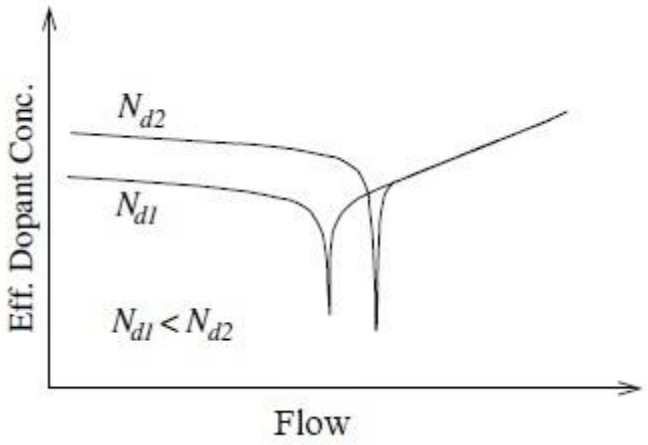

Figure 2.17 – Dependence of particle flow on effective dopant concentration in a silicon detector with two different initial donor concentrations [2]

Depletion Voltage

Generally, radiation detecting photodiodes are operated in fully depleted mode. The bias voltage is kept at several tens of volts above the depletion voltage to ensure complete depletion.

However, with prolonged irradiation, the depletion voltage increases, requiring increase in bias voltage. The main consequence is the change in effective dopant concentration due to radiation damage.

To overcome this effect, bias voltage has to be increased.

Charge Trapping and Carrier Lifetime

Charge collection efficiency of the electrodes is directly proportional to the number of free charges available. Perhaps the worst effect that incident radiation can cause in a semiconductor detector is the creation of energy levels that trap the charges for a long time. These could be either electron traps or hole traps, according to whether they are near the valence band or conduction band respectively.

If a charge recombines, it can no longer contribute to the current and causes a nonlinearity in the detector's response. Note that the net result of traps is a decrement in the average carrier lifetime in the bulk of the material.

3 – Materials and Methods

3.1 Detectors' Structure

The devices used in this work are OTFTs (Organic Thin Film Transistors), fabricated on a polyethylene terephthalate (PET) substrate.

The advantages of using such a material are noteworthy: it is flexible, which allows the application of the finished devices of irregular surfaces; it is inexpensive, so it offers easy up-scaling opportunities; it can be obtained at relatively low temperatures; it is 3-D printable, which opens many application possibilities.

The aluminium gate is deposited by thermal evaporation and then coated with a 6 nm Al_2O_3 layer, realized at room temperature by UV-Ozone oxidation.

Parylene C is deposited by chemical vapour deposition (CVD), using A174 as adhesion promoter. The thickness of the Parylene layer is 25 nm.

The electrodes and the dielectric layer have been fabricated at the University of Cagliari, while the semiconductor layer has been deposited here at the University of Bologna.

Thanks to the ease of the dielectric fabrication process, such a procedure can be very simply up-scaled to an industrial size. In fact, the employed procedure for Al_2O_3 growth can be performed at low costs over relatively large areas and, in addition, many other methods are available for aluminium oxidation. Furthermore, even if parylene C deposition requires a dedicated instrumentation, it is already widely employed in several industrial processes for the deposition of insulating films of different thicknesses (from tens of nm up to tens of μm), with excellent properties in terms of reproducibility and quality.

Thermally evaporated gold source and drain electrodes are realized on top of the parylene layer with a photolithographic process. They have an interdigitated structure in order to maximize the conduction channel's dimensions.

The two organic semiconductors are DiF-TES-ADT and DiF-TEG-ADT, which are applied to the device by drop-casting in a solution using Chlorobenzene as a solvent. Deposition is performed at room temperature, and then the samples are left to rest for two hours. Figure 3.1 show a representation of the samples' structure. Drop-casting is chosen in order to gives rise to high-quality micro-crystalline films.

The conduction channel's dimensions are:

- Length L = 45 μm (distance between interdigitated electrodes)
- Width W = 50 000 μm (this relatively big width is obtained thanks to the electrodes' structure).

It should be noted that a very high gate dielectric capacitance is obtained (18 nF/cm^2); this allows to work with very low operating voltages, lower than 2V.

This fabrication technique is simple, very inexpensive and easily up-scalable to industrial production. [19]

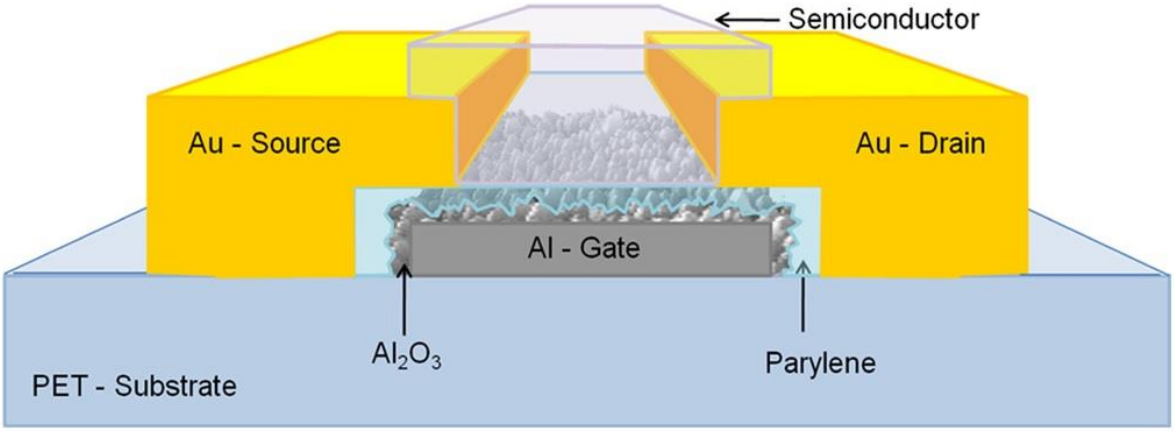

Figure 3.1 - Schematic representation of OTFT's structure [19]

3.2 Sample Fabrication Process

Firstly, each sample is secured to a microscopic slide.

Secondly, the organic solution is prepared and stirred for approximately 10 minutes; 3µL of the solution are then deposited onto the electrodes by SAC drop-casting; in the next few hours, solvent gradually evaporates from the component leaving a layer of the organic molecules.

Once the solvent has completely evaporated, the sample is wired using conductive silver paint. [1][19]

3.2.1 Solutions' composition

In order to study how different organic molecules affect the devices' detecting properties, two different crystalline organic semiconductors are chosen as solutes:

- **DiF-TES-ADT** (Figure 3.2 a)
  DiF-TES-ADT is a soluble, organic semiconductor for printed and flexible electronic applications with the following properties:

  Molecular formula: $C_{34}H_{36}F_2S_2Si_2$
  Molecular weight: 602.949 g/mol

- **DiF-TEG-ADT** (Figure 3.2 b)
  DiF-TEG-ADT is the germanium-based counterpart of the DiF-TES-ADT.

  Molecular formula: $C_{34}H_{36}F_2S_2Ge_2$
  Molecular weight: 692.039 g/mol

Both these crystalline organic molecules are soluble and offer versatile processing possibilities.

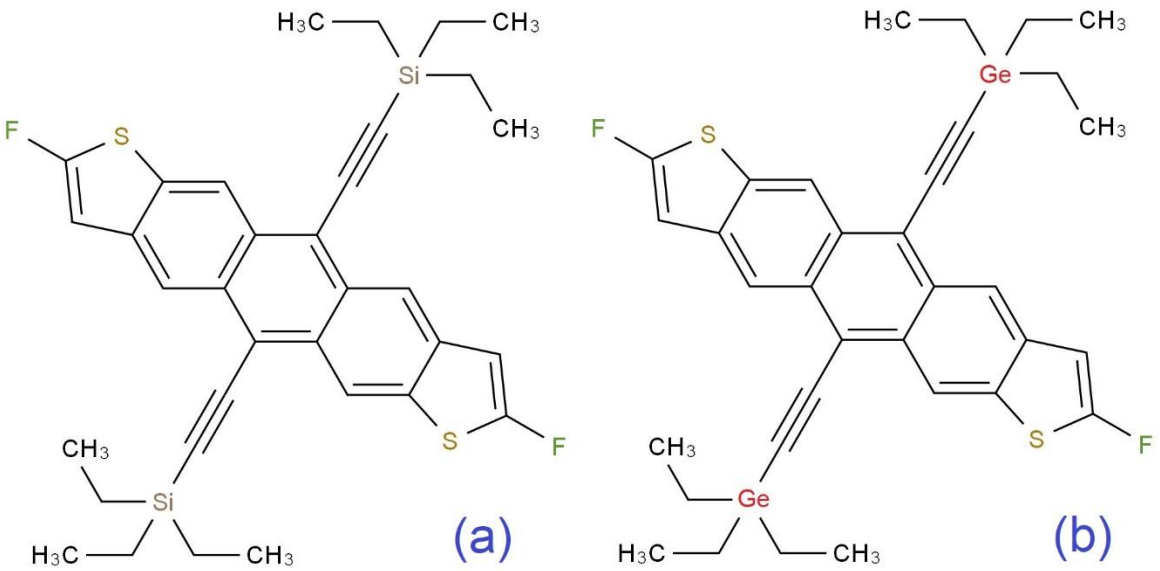

Figure 3.2 – Molecular structures of DiF-TES-ADT (a) and DiF-TEG-ADT (b) [7]

For both solutions, the chosen solvent is Chlorobenzene.
Chlorobenzene is an aromatic organic compound with the chemical formula C_6H_5Cl (Figure 3.3). It is a common, colorless and flammable solvent, also used to obtain other chemicals.

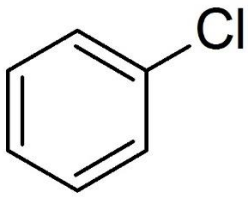

Figure 3.3 – A Chlorobenzene molecule [7]

3.2.2 Solutions' deposition method

The solutions are deposited onto the samples by drop-casting.

The organic molecules are mixed with a suitable solvent, which must prevent the material from changing its form, and cast by dropping on the target substrate.

The main advantage of this technique is its simplicity; on the other hand, it is not easy to obtain uniform coating and thickness.

Drop-casting can be performed in two different environments.

The first environment is a standard, ventilated laboratory condition.

The second environment is saturated with the solvent's molecules; the saturated environment prevents the solvent from evaporating too quickly, allowing the solute's molecules to better align with one another.

This should minimize crystal defects and maximize sensitivity; crystal imperfections and impurities produce intermediate energy levels that greatly enhance the recombination process, compromising the sample's conductivity.

This latter method is called SAC Method. [21][22]

I therefore drop-cast the solutions in SAC conditions; the detecting properties will then be compared to the ones previously obtained with different techniques.

3.3 Electrical Characterization

Once the devices are completed, they are tested on a probe station to verify the operation conditions of the underlying electrical components (Figure 3.4).

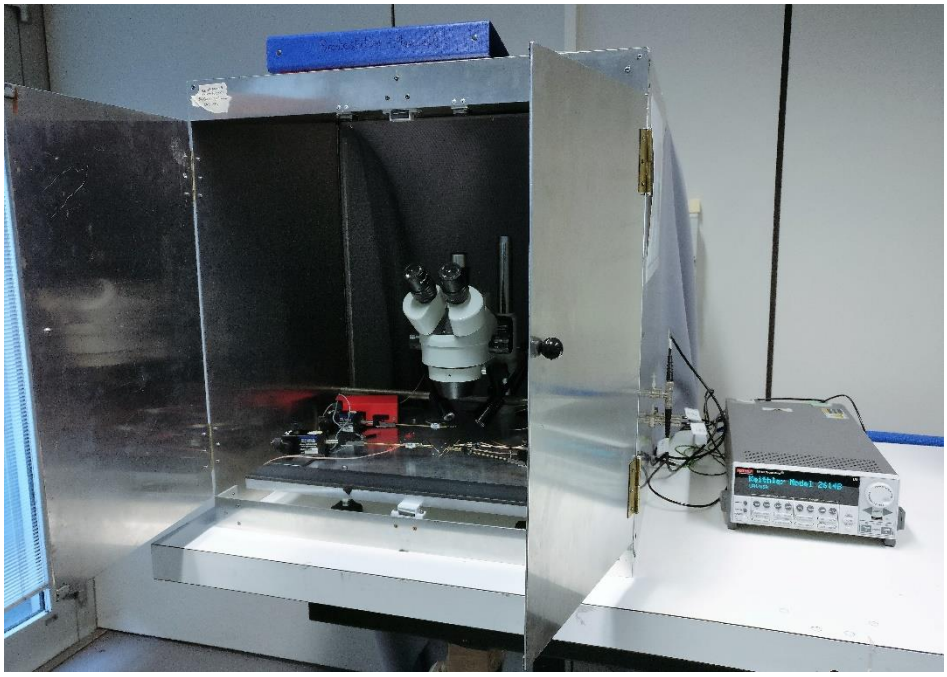

Figure 3.4 – Probe station

The probe station has the following specifications:

- Faraday cage enclosure to guarantee maximum isolation from any external source
- Optika ST111 microscope
- Keithley 2614B dual channel SourceMeter (Figure 3.5)

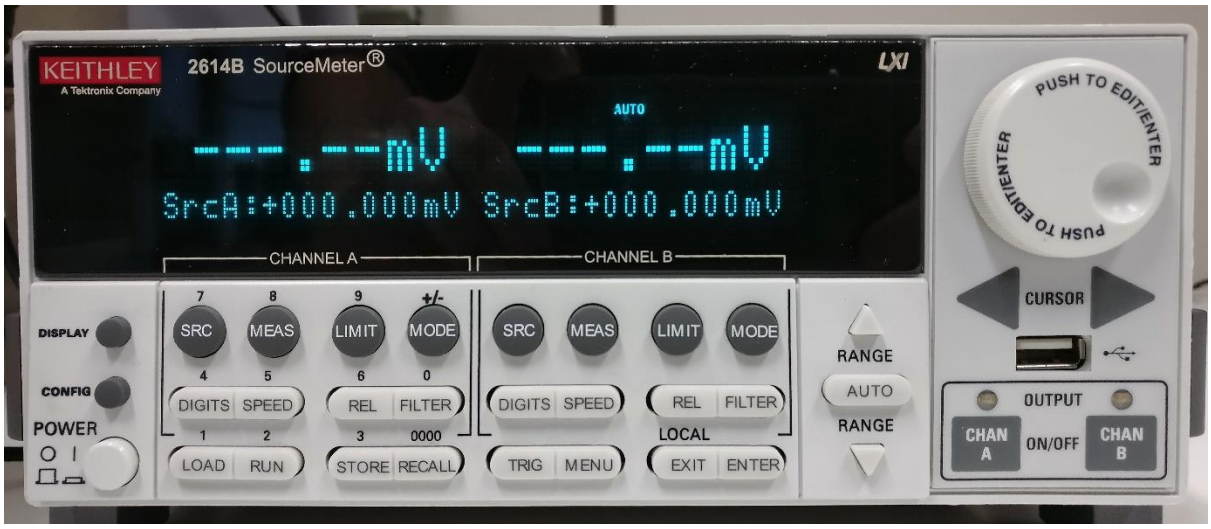

Figure 3.5 – Keithley 2614B dual channel SourceMeter

The SourceMeter's accuracy specifications are reported in Table 3.1:

Voltage measurement accuracy	
Range	Accuracy at T = (23±5)°C
100 mV	0.015% + 150 µV
1 V	0.015% + 200 µV
6 V	0.015% + 1 mV
40 V	0.015% + 8 mV
Current measurement accuracy	
Range	Accuracy at T = (23±5)°C
100 nA	0.05% + 100 pA
1 µA	0.025% + 500 pA
10 µA	0.0.25% + 1.5 nA
100 µA	0.02% + 25 nA
1 mA	0.02% + 200 nA

Table 3.1 – Accuracy specifications of Keithley 2614B dual channel SourceMeter

Electrical characterization is performed, with a custom made Labview acquisition program, in three different conditions to verify the devices' condition.
First, a linear transfer characterization is performed.
Thereafter, the transfer properties in saturation conditions are studied.
Lastly, the output characteristics are analysed for various values of V_g.
The characterization's electrical connections are outlined in Figure 3.6. [20]

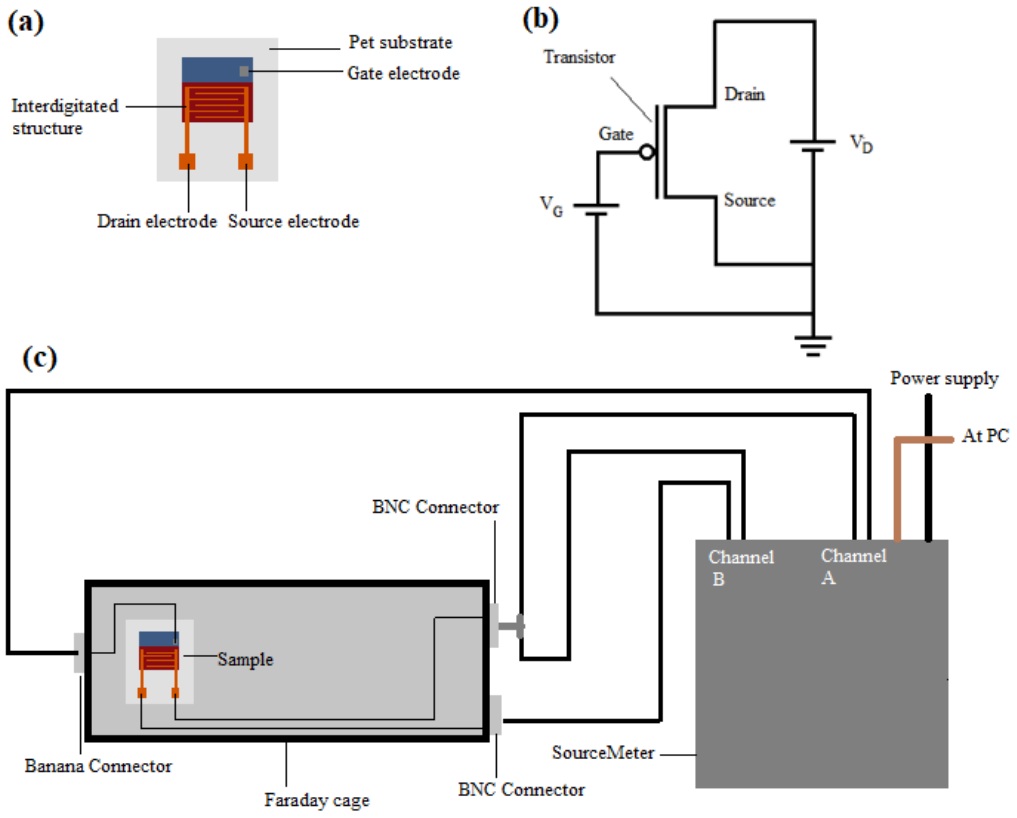

Figure 3.6 – Electrical connections between the sample and the SourceMeter [20]

3.4 X-ray Characterization

After the electrical characterization, the samples are tested under the exposure of X-rays, emitted by an X-ray tube.

One at a time, the samples are mounted into a sample holder, which shields the samples from visible light and acts also as a Faraday cage, and connected to a SourceMeter (Keithley 2614B, see Figure 3.5 above) with the same connections used during electrical characterization.

The sample holder is then secured inside a lead glass structure, aligned to the X-ray beam (Figure 3.10).

The X-ray tube is connected to an adjustable generator; operating on the generator, different dose rates can be obtained.

The X-ray tube is a Mo-tube (K_α=17.5 keV, model PANalytical2 PW 2285/20), which operates at a voltage of 35 kV and at the current defined by the user in the range 5 mA ÷ 30 mA. Its spectrum is reported in Figure 3.7.

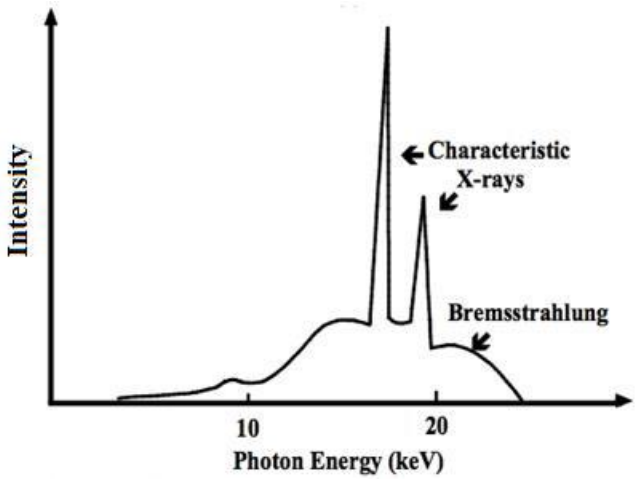

Figure 3.7 – energy spectrum of the Mo-tube [20]

The Mo X-ray tube was previously calibrated employing the *Barracuda* radiation detector (RTI Group, Sweden, Figure 3.8).

Figure 3.8 – Barracuda radiation detector used to calibrate the Mo-tube [20]

The calibration results are reported in Table 3.2. The current I indicates the current on the X-ray tube, and in the plot this current is reported as a function of the dose-rate measured by the *Barracuda* probe rescaled for the sample-tube distance (D_{re}).

The SI unit for absorbed radiation is the gray (Gy), which is defined as the absorption of one joule of radiation energy per kilogram of matter: [20]

$$1\ Gy = 1\ \frac{J}{Kg} = 1\ \frac{m^2}{s^2} \tag{3.1}$$

I [mA]	Dose rate [mGy/s]
5	4.6 ± 0.2
10	10.2 ± 0.5
15	14.5 ± 0.7
20	20 ± 1
25	24 ± 1
30	30 ± 1

Table 3.2 – Calibration results

3.4.1 X-ray exposure

The exposure cycle is dynamic, with alternating exposure and dark phases of equal time, managed by a shutter on the X-ray emitter; for each data acquisition, three on-off cycles of 120 seconds each are executed.

The X-ray Mo-tube was fixed at the distance of 33 cm from the studied device, which was irradiated with X-ray beams having different dose rates.

It should be noted that the potential on the generator is kept at the same value for every current value, in order to modify the dose rate without affecting the energy of the radiation emitted. [20]

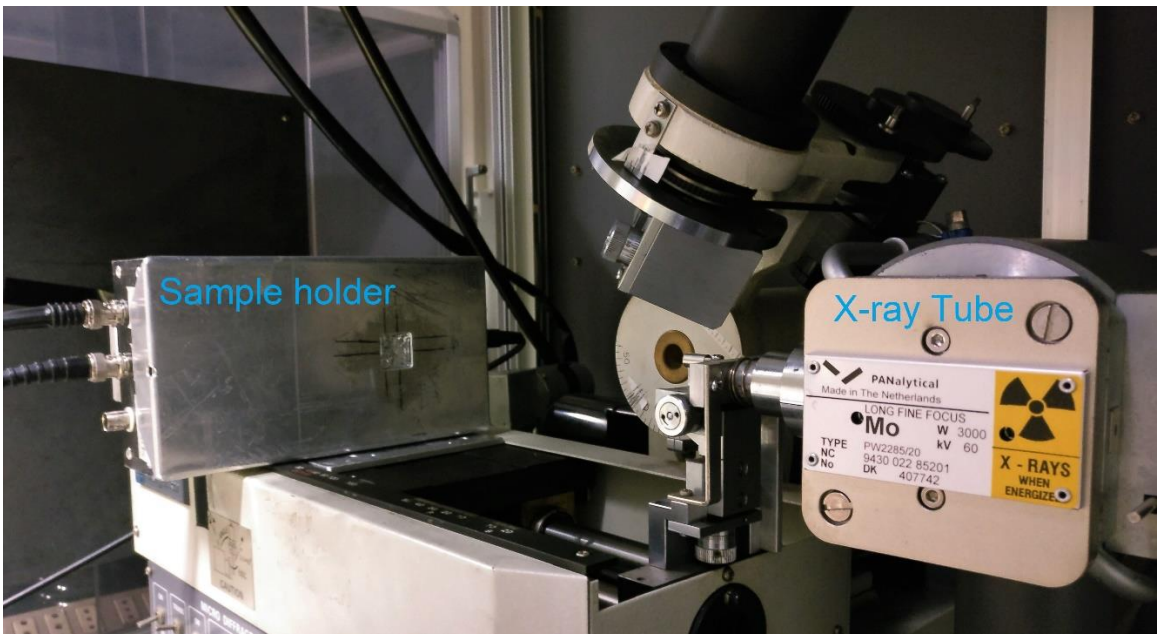

Figure 3.10 – X-ray characterization equipment

3.4.2 X-ray exposure effects analysis

In order to check the X-ray exposure's effects on the samples, linear and saturation transfer characterizations are performed before and after the exposure; data is then compared.

A difference between the two is expected, with lower maximal current reached on the test executed after the exposure; this is caused by the damaging effects of radiation exposure, namely atomic displacement, which causes irregularities in the lattice, and lattice excitation, both affecting the sample's conductivity.

3.4.3 Data analysis parameters

Shown below are the parameters needed for a complete data analysis and detector's quality evaluation.

Photocurrent

The photocurrent is the current generated by the interaction with incident ionizing radiation.

It is easily calculated from the collected data as the difference between exposure current I_{ON} and dark current I_{OFF} of each on-off cycle averaged:

$$\Delta I = \frac{1}{N}\sum_{i=1}^{N}(I_{ON} - I_{OFF}) \tag{3.2}$$

where N is the number of peaks considered.

As time passes between one exposure and the next one, dark and exposure currents decrease because of the bias stress. To compensate for this phenomenon, it is necessary to normalize the curve, subtracting the linear fit of the dark current values to all the data collected.

With this expedient, it becomes easy to study the photocurrent alone, excluding other factors.

Sensitivity S

It is defined as the ratio between photocurrent and dose rate:

$$Sensitivity = \frac{Photocurrent}{Dose\ rate} \tag{3.3}$$

It should be noted that there is linear relation between the dose rate and the photocurrent.

Therefore, to obtain a more accurate measure of the sensitivity, a linear fit of photocurrent as a function of dose rate is executed; the sensitivity is then the slope of the fitting line.

Sensitivity is the main parameter in determining a detector's quality, since a good detector should provide a high photocurrent with a low dose rate.

4 – Results

4.1 Samples

I now present the obtained results. Shown below (Table 4.1) are the samples' name and fabrication specifications.

Name	Molecule	Solution's specifications	Conc.	Deposition method
TES_S1	DiF_TES_ADT	Solute: 0.00107 g Solvent: 200 µL	0.5%	SAC
TES_S2				SAC
TEG_S3	DiF_TEG_ADT	Solute: 0.00113 g Solvent: 200 µL	0.5%	SAC
TEG_S4				SAC

Table 4.1 – Samples' specifications

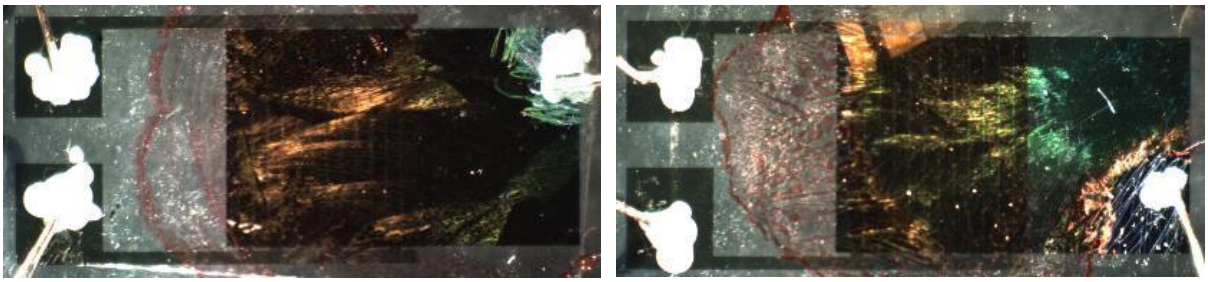

Figure 4.1 – DiF-TES-ADT Sample TES_S2 (left) and DiF-TEG-ADT Sample TEG_S3 (right)

4.2 Electrical Characterization

Shown below are the electrical characterization graphics obtained for all samples.
For every sample, the parameters used for the characterization are:

- **Linear transfer**
  V_D = -0.2 V
  V_g = [-3; 3] V, with discrete 0.2 V steps

- **Saturation transfer**
  V_D = -3 V
  V_g = [-3; 3] V, with discrete 0.2 V steps

- **Output**
  V_D = [-4; 0] V, with discrete 0.2 V steps
  V_g = (-5, -3, -2, -1, 0, 1, 3, 5) V

It should be noted that the parameters indicated above and the obtained characteristics relate to p-type semiconductors.

4.2.1 Samples TES_S1-TES_S2

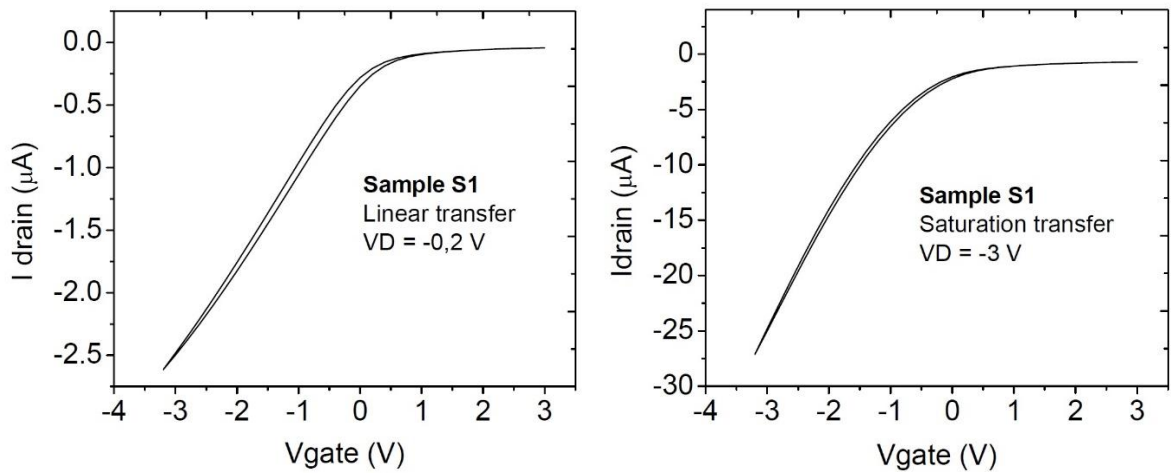

Figure 4.2 – Linear (left) and Saturation (right) transfer characteristics of TES_S1

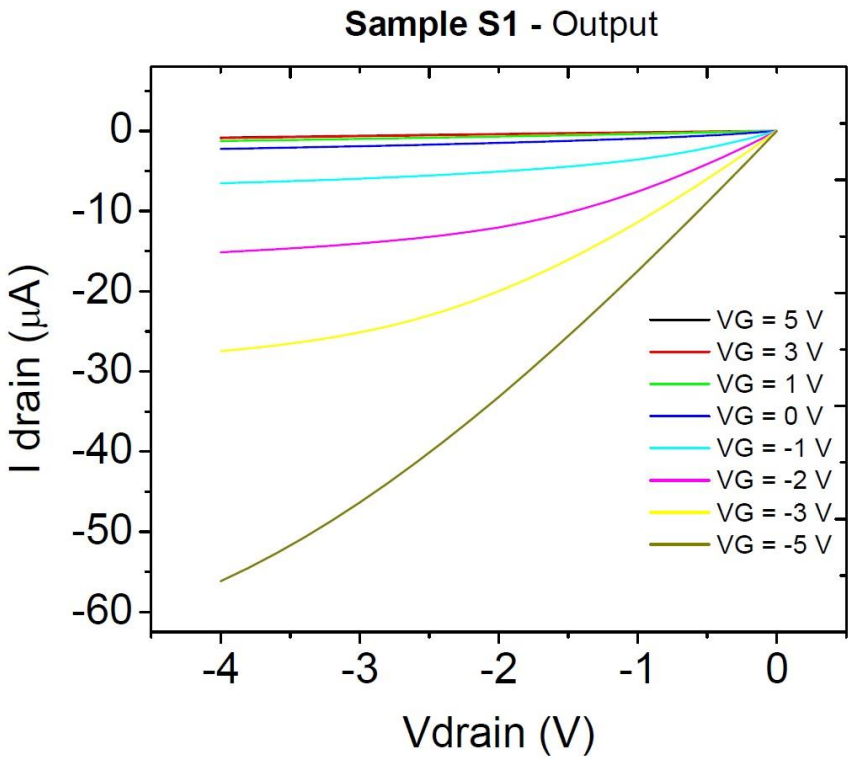

Figure 4.3 – Output characteristics of TES_S1

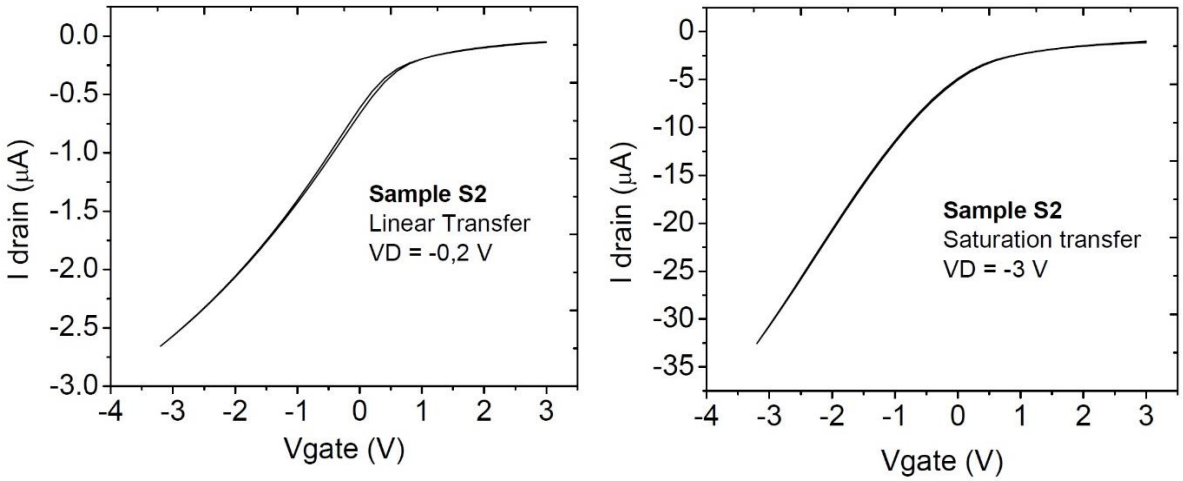

Figure 4.4 - Linear (left) and Saturation (right) transfer characteristics of TES_S2

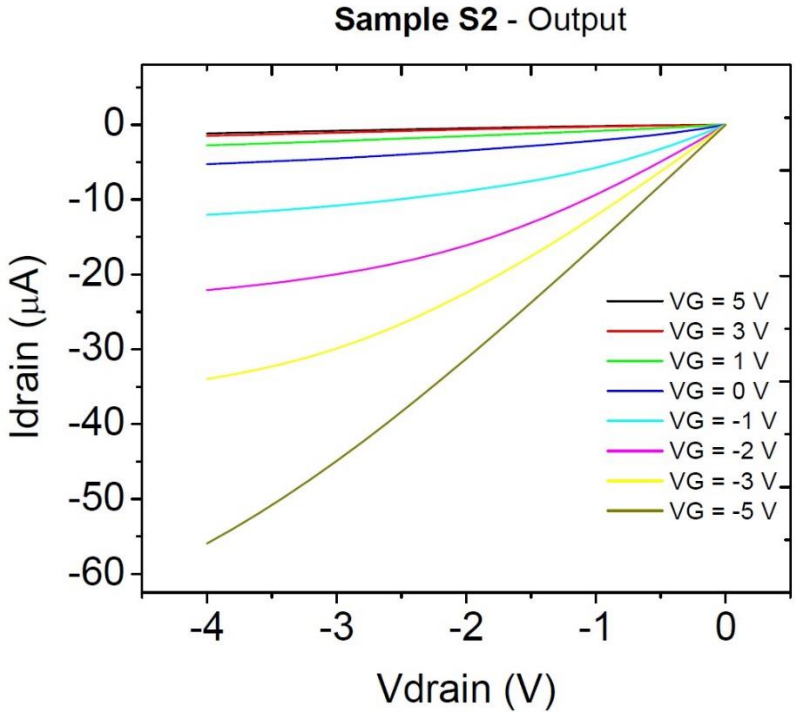

Figure 4.5 – Output characteristics of TES_S2

Table 4.2 shows the electrical parameters obtained with the above-mentioned characterizations.

Sample	Mobility μ_{SAT} [$cm^2/V \cdot s$]	V_{th} [V]	On/off ratio
TES_S1	$1.59 \cdot 10^{-1}$	0.96	$3.8 \cdot 10$
TES_S2	$1.14 \cdot 10^{-1}$	2.21	$2.9 \cdot 10$

Table 4.2 – Electrical parameters. These results only refer to the saturation region.

Samples TES_S1 and TES_S2 have good electrical performances; furthermore, they show good stability and they do not have hysteresis in the transfer curve.

4.2.2 Samples S3-S4

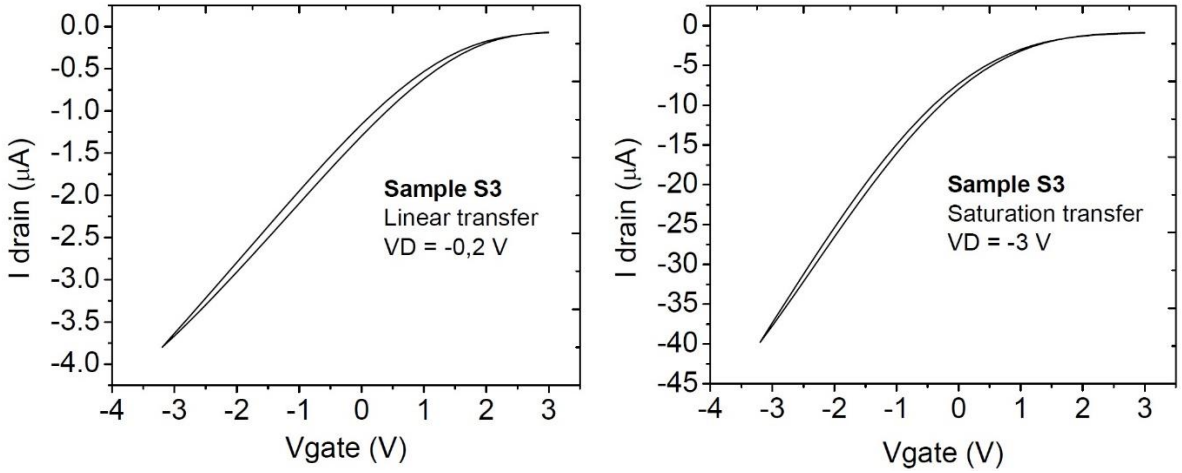

Figure 4.6 - Linear (left) and Saturation (right) transfer characteristics of TEG_S3

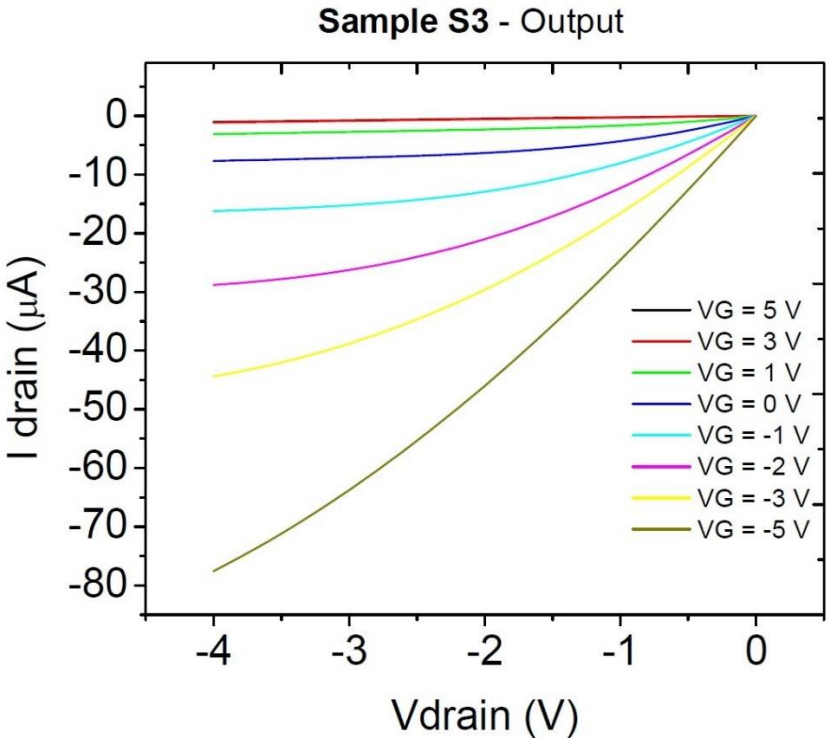

Figure 4.7 – Output characteristics of TEG_S3

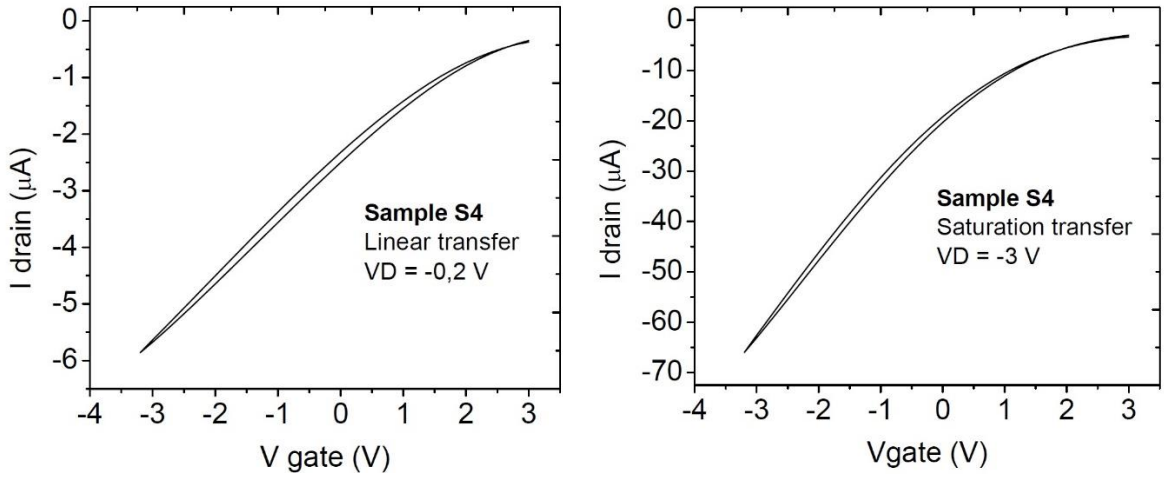

Figure 4.8 - Linear (left) and Saturation (right) transfer characteristics of TEG_S4

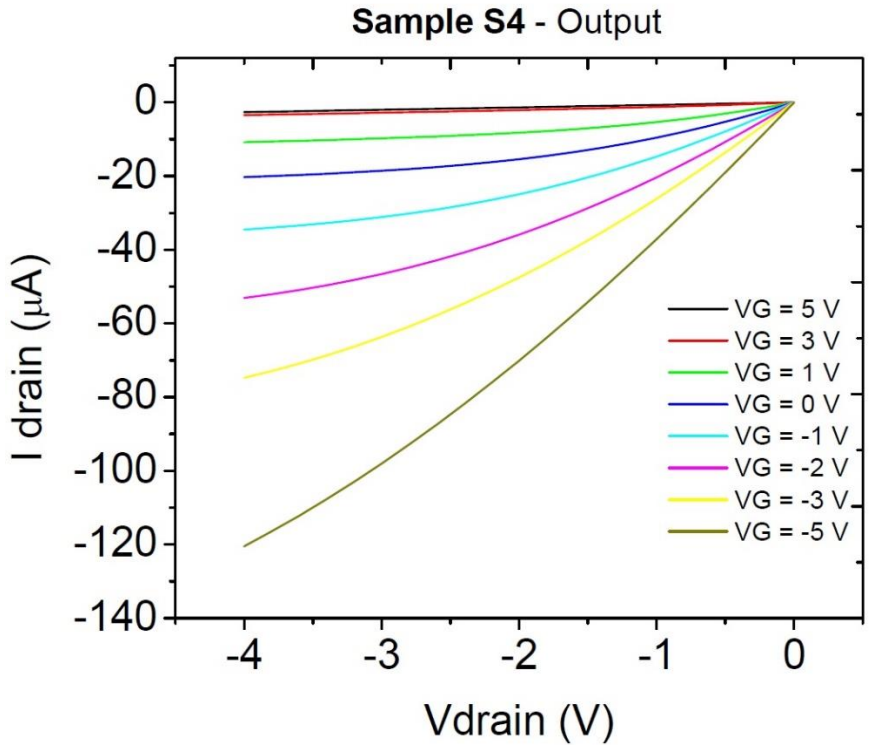

Figure 4.9 – Output characteristics of TEG_S4

Table 4.3 shows the electrical parameters obtained with the above-mentioned characterizations. All the results obtained were congruent to what I expected.

Sample	Mobility μ_{SAT} [$cm^2/V \cdot s$]	V_{th} [V]	On/off ratio
TEG_S3	$1{,}69 \cdot 10^{-1}$	2,43	$4{,}6 \cdot 10$
TEG_S4	$1{,}37 \cdot 10^{-1}$	3,79	$2{,}2 \cdot 10$

Table 4.3 – Electrical parameters

Samples TEG_S3 and TEG_S4 have good electrical performances; furthermore, they show good stability and they do not have hysteresis in the transfer curve. They behave in a way very similar to the TES samples.

4.3 X-ray Characterization

The photocurrent is generated by the interaction with incident ionizing radiation.

As time passes between one exposure and the next one, dark and exposure currents decrease because of the bias stress.

To compensate for this phenomenon, it is necessary to normalize the curve; this is done by subtracting the linear fit of the dark current values to all the data collected.

With this expedient, it becomes easier to visualize the variations in the current I_D caused by the incoming radiation.

Once the curve is normalized, it is possible to calculate the average photocurrent between every on-off cycle. For every cycle, the photocurrent's chosen value is in the saturation point of the interaction between radiation and matter.

With every value of the average photocurrent, the sensitivity is easily calculated from the linear fit of the photocurrent as a function of the dose rate (Figure 4.11). The sensitivity is in fact the slope of the fitting line.

Shown below are the X-ray exposure graphics; it should be noted that the yellow zones indicate exposure phases, while the white zones indicate dark phases.

For every test, I chose cycles composed by 60 seconds of exposure followed by 60 seconds of dark.

4.3.1 Samples TES_S1-TES_S2

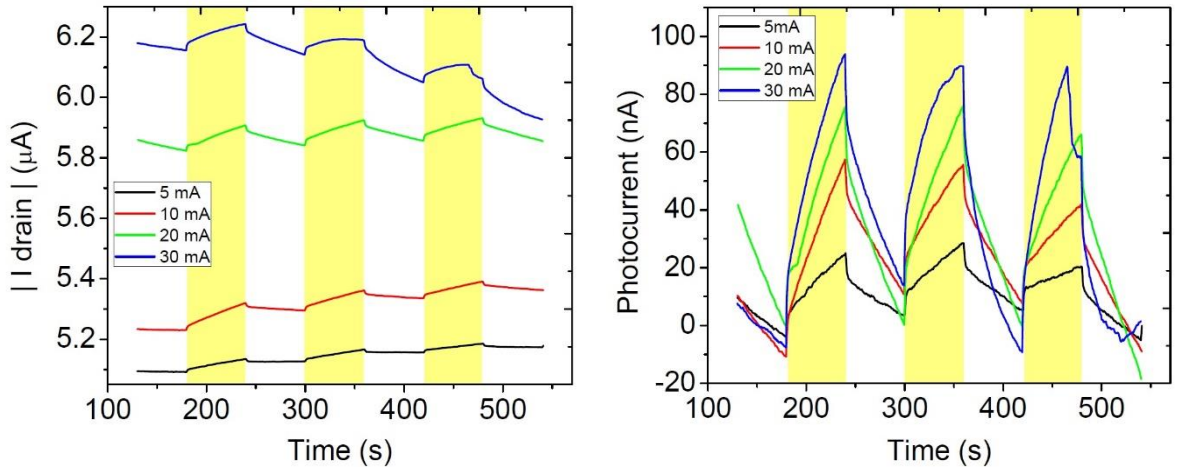

Figure 4.10 – X-ray exposure current I_D before (left) and after (right) the normalization of sample TES_S1

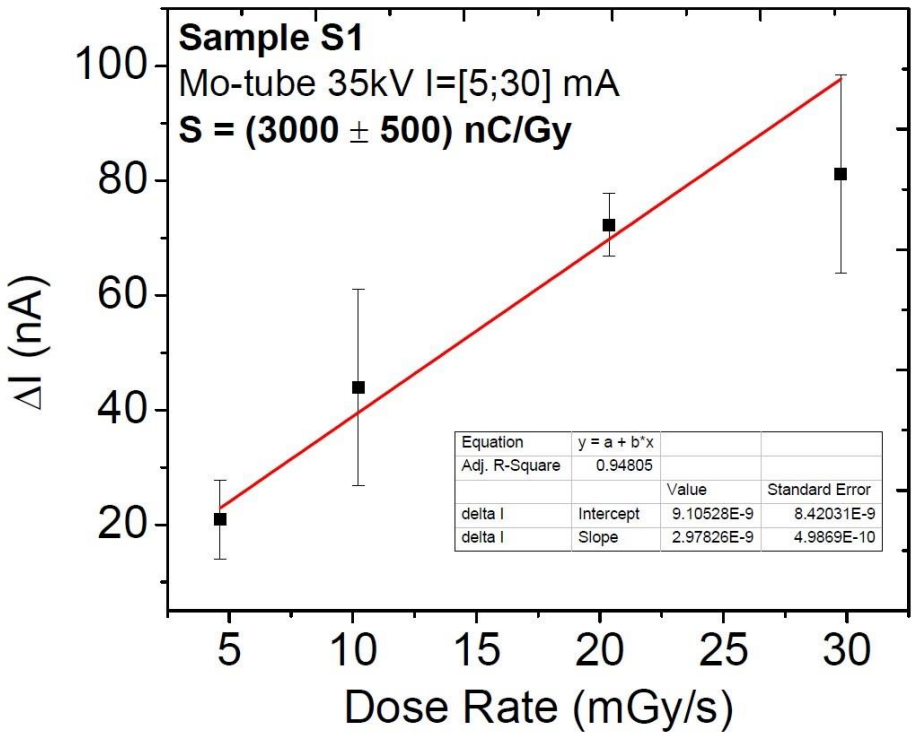

Figure 4.11 – Linear fit of the photocurrent of TES_S1 as a function of the dose rate

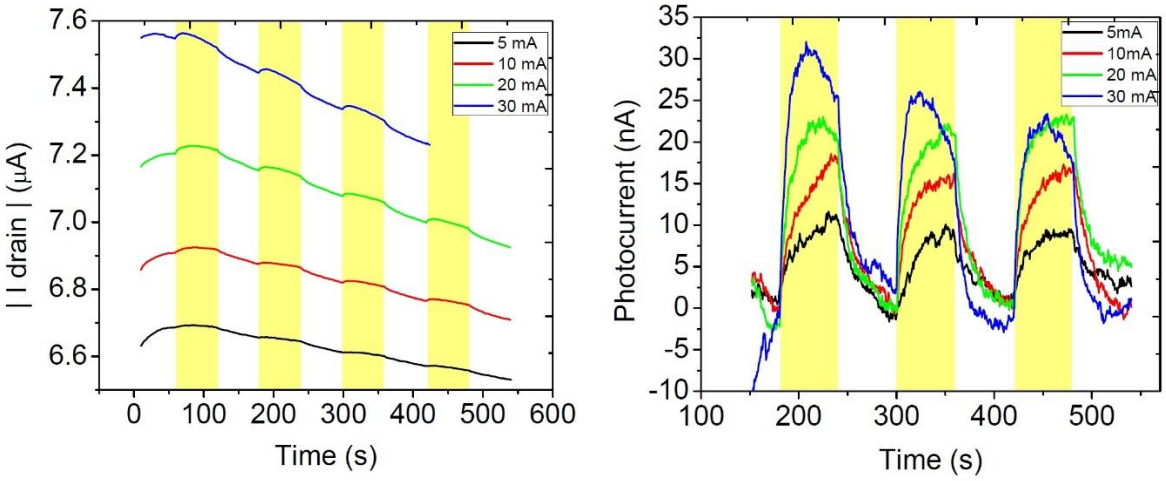

Figure 4.12 - X-ray exposure current I_D before (left) and after (right) the normalization of sample TES_S2

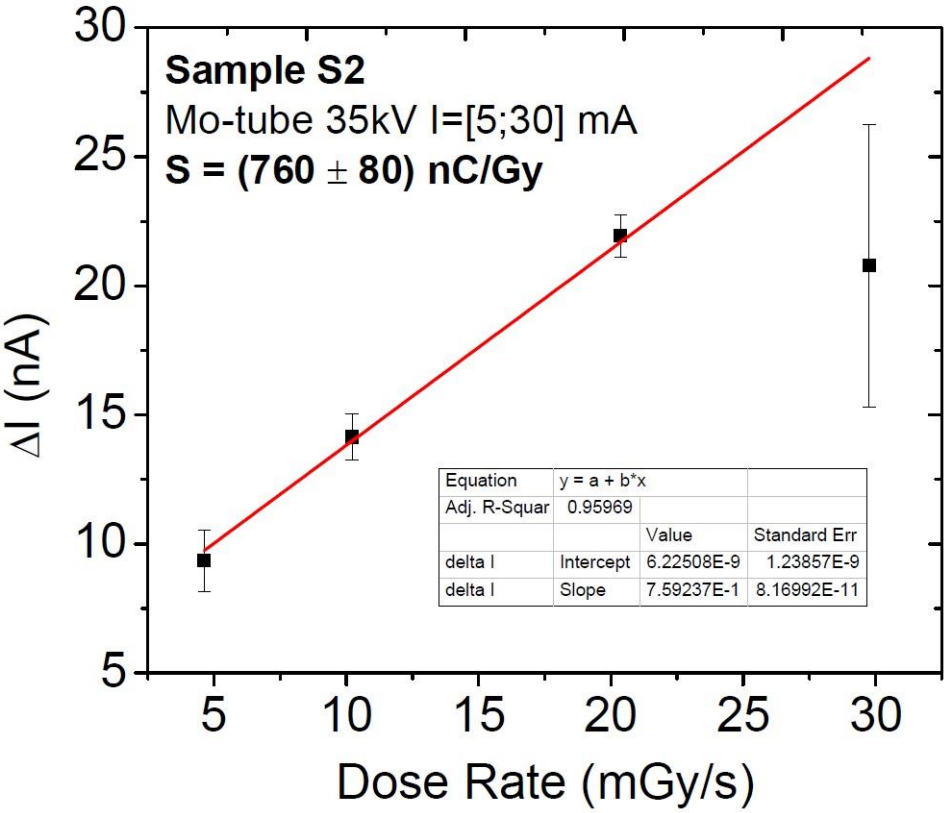

Figure 4.13 – Linear fit of the photocurrent of TES_S2 as a function of the dose rate

It should be noted how the response of the samples to the exposure, in terms of drain current I_D, is linear to the applied dose rate, just as expected (Figure 4.11, 4.13).

This proves the assumptions made on the samples' behaviour.

The photocurrent obtained with a 30 mGy/s dose rate on sample TES_S2 is quite different from the other three (Figure 4.13). This is probably due to the stress caused on the sample by the high dose rate; furthermore, the higher dose rate was the last tested, so the sample had already accumulated some stress from the previous expositions.

Table 4.4 shows the parameters obtained for samples TES_S1 and TES_S2.

Sample	V_g [V]	V_D [V]	X-ray tube settings	Sensitivity [nC/Gy]
TES_S1	-2	-3	35 kV , [5;30] mA	(3000 ± 500)
TES_S2	-2	-3	35 kV , [5;30] mA	(760 ± 80)

Table 4.4 – X-ray exposure parameters. The transistor is kept at these values of V_g and V_D in order to be in accumulation mode; this value of V_g is chosen because, in previous evaluations at DIFA – University of Bologna, it was to be the one that provides the highest sensitivity

The sensitivities of both samples are outstanding, much higher than regular drop-casting or spin-coated TES and TEG molecules; furthermore, they are better than drop-casted TIPS pentacene and comparable with drop-casted TIPGe pentacene.

All these comparison values were previously obtained at DIFA (Physics and Astronomy Department - University of Bologna).

It becomes even more significant if we consider that TIPGe pentacene is germanium-based, and should be far superior to the silicon-based molecules in terms of sensitivity, because of the higher Z-number. [20]

This is particularly interesting and shows that the SAC deposition method is very promising for this type of molecule.

4.3.2 Samples TEG_S3-TEG_S4

Thanks to their germanium-based DiF-TEG-ADT molecules, samples TEG_S3 and TEG_S4 should show even higher sensitivity values.

Unfortunately, problems were encountered during the molecule's deposition, therefore the samples behaved in an anomalous way when exposed to X-rays and the exposure characteristics did not meet the required standards.

4.3.3 Damaging X-ray effects

As described in section 3.4.2, linear and saturation transfer characteristics are obtained before and after X-ray exposure; this is done in order to analyse the effects of radiation exposure on the samples (Figure 4.14).

A difference between the two is expected, with lower maximal current reached on the test executed after the exposure; this is caused by the damaging effects of radiation exposure, namely atomic displacement, which causes irregularities in the lattice, and lattice excitation, both affecting the sample's conductivity.

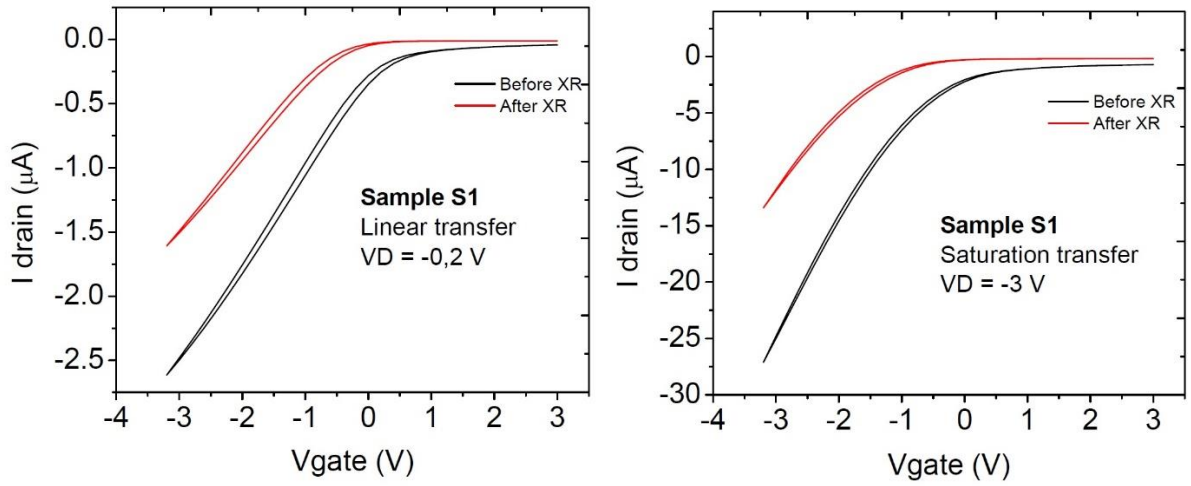

Figure 4.14 – Linear (left) and saturation (right) transfer characteristics of TES_S1

As expected, a slight degradation in the detectors' characteristics is found for both the linear transfer and the saturation transfer.

5 – Conclusions

The detection of ionizing radiations is a rapidly growing research area, offering many development opportunities.

Organic semiconductors are becoming more and more popular in radiation detection, thanks their good detection properties, flexibility and very low working voltage.

To this day, they have mainly been used as scintillators or as photodiodes, but in recent years their application as direct radiation detectors made many steps forward.

In this study, I wanted to further develop our knowledge about these devices in direct detection conditions, in particular observing how the detector's sensitivity is influence by two factors: the organic molecule of choice and its deposition technique.

Therefore, I created two organic solutions, with DiF-TES-ADT and DiF-TEG-ADT as solutes and chlorobenzene as a solvent, and I drop-casted them on four transistors in SAC conditions.

Successively, I tested their electrical operation and I exposed them to ionizing radiations of the X-ray spectrum, using alternated exposure and dark phases.

We now compare the results deduced with the new SAC method with values of other deposition methods previously obtained at the DIFA (Physics and Astronomy Department) – University of Bologna:

Sample	**Molecule, solvent and concentration**	**Deposition method**	**μ_{SAT} [$cm^2/V \cdot s$]**	**V_{th} [V]**	**Sensitivity [nC/Gy]**
TES_S1	DiF-TES-ADT chlorobenzene 0.5%	SAC Drop-casting	$1.59 \cdot 10^{-1}$	0.96	(3000 ± 500)
TES_S2			$1.14 \cdot 10^{-1}$	2.21	(760 ± 80)
TEG_S3	DiF-TEG-ADT chlorobenzene 0.5%		$1{,}69 \cdot 10^{-1}$	2.43	-
TEG_S4			$1{,}37 \cdot 10^{-1}$	3.79	-
P1	TIPS pentacene tuolene 0.5%	Drop-casting (no SAC)	$8 \cdot 10^{-2}$	0.4	(960 ± 70)
P2	TIPGe pentacene tuolene 0.5%		$6 \cdot 10^{-2}$	-	(3080 ± 20)
P3	DiF-TES-ADT chlorobenzene 1.2%	Spin-casting	$3.26 \cdot 10^{-3}$	-0.14	(20 ± 6)
P4	DiF-TEG-ADT chlorobenzene 1.2%		$2.61 \cdot 10^{-2}$	0.66	(300 ± 100)

Table 4.5 – Comparison between the newly fabricated samples and previously obtained results. It should be noted that the properties of lines P1, P2, P3 and P4 are the average between all the samples fabricated with those specifications.

For all samples listed in Table 4.5, the operation voltages are V_D = -3V, V_g = -2V.

The sensitivity values obtained with DiF-TES-ADT are comparable to the ones previously obtained with TIPGe pentacene, which is a germanium-based molecule with very high sensitivity. [20]

Unfortunately, I was not able to obtain acceptable results with the germanium-based molecules, most probably due to some issues in the deposition process.

However, the excellent sensitivities of the silicon-based detectors indicate that good results can be achieved for the germanium-based detectors, too, if further analysis is performed to identify deposition corrections that could be made.

Nevertheless, I can safely say that the new deposition method is promising and, with further analysis, could possibly lead to even higher performances.

References

[1] Laura Basiricò, Andrea Ciavatti, Tobias Cramer, Piero Cosseddu, Annalisa Bonfiglio & Beatrice Fraboni, "*Direct X-ray photoconversion in flexible organic thin film devices operated below 1V"*. nature communications 13063 (2016)

[2] Syed Naeem Ahmed, *"Physics and Engineering of Radiation Detection"*, Academic Press (2007)

[3] Hofmann, A. W. *"On Insolinic Acid"*, Proceedings of the Royal Society *(1855)*

[4] *"Bonding in benzene – the Kekulé structure".* www.chemguide.co.uk *(2015)*

[5] *"Chemical Reactivity"* www.chemistry.msu.edu *(2015)*

[6] Thiele, Johannes *"Zur Kenntnis der ungesättigten Verbindungen"* ([Contribution] to our knowledge of unsaturated compounds). Justus Liebig's Annalen der Chemie (1899)

[7] IUPAC Gold Book – *conjugated system (conjugation)*

[8] March Jerry, *"Advanced Organic Chemistry reactions, mechanisms and structure"* (3rd edition) New York: John Wiley & Sons, inc. (1985)

[9] Holger F. Bettinger*, "Electronic structure of higher acenes and polyacene: The perspective developed by theoretical analyses".* Pure Appl. Chem., Vol. 82, No. 4, pp. 905–915

[10] The Nobel Prize in Chemistry, 2000: Conductive polymers, https://www.nobelprize.org/

[11] Herbert Naarmann, *"Polymers, Electrically Conducting"* in Ullmann's Encyclopedia of Industrial Chemistry Wiley-VCH, Weinheim (2002)

[12] Colin Reese, Mark Roberts, Mang-mang Ling, and Zhenan Bao, *"Organic thin film transistors"*. Department of Chemical Engineering, Stanford University, 381 North South Mall, Stanford, CA 94305-5025 USA (2004)

[13] Ilaria Fratelli, *"Flexible oxide thin film transistors: device fabrication and Kelvin probe force microscopy analysis"*. Alma Mater Studiorum – University of Bologna (2016)

[14] Beatrice Fraboni, Andrea Ciavatti, Laura Basiricò and Alessandro Fraleoni-Morgera, *"Organic semiconducting single crystals as solid-state sensors for ionizing radiation"*. Faraday discussions DOI: 10.1039/c4fd00102h (2014)

[15] Cox, James F., "Fundamentals of linear electronics: integrated and discrete". Cengage learning

[16] Filip Tavernier and Michiel Steyaert, “High-speed optical receivers with integrated photodiode in nanoscale CMOS”. Springer

[17] Photodiode Technical Guide on http://www.hamamatsu.com/us/en/

[18] F.G. Knoll, “Radiation detection and measurement” (4th edition). Wiley ed., Hoboken, NJ

[19] P. Cosseddu, S. Lai, M. Barbaro, and A. Bonfiglio, *“Ultra-low voltage, organic thin film transistors fabricated on plastic substrates by a highly reproducible process”*. Appl. Phys. Lett. 100, 093305 (2012); doi: 10.1063/1.3691181

[20] Tommaso Neri, *“Novel organic semiconducting small molecules for X-ray detection”*. Alma Mater Studiorum – University of Bologna (2017)

[21] Peter J. Diemer, Jacori Hayes, Evan Welchman, Rawad Hallani, Sujitra J. Pookpanratana,Christina A. Hacker, Curt A. Richter, John E. Anthony, Timo Thonhauser,and Oana D. Jurchescu, *“The influence of isomer purity on trap states and performance of organic thin-film transistors”.* Advanced Science news (2016)

[22] Yaochuan Mei, Marsha A. Loth , Marcia Payne , Weimin Zhang, Jeremy Smith, Cynthia S. Day , Sean R. Parkin , Martin Heeney , Iain McCulloch, Thomas D. Anthopoulos , John E. Anthony , and Oana D. Jurchescu, *“High mobility field-effect transistors with versatile processing from a small-molecule organic semiconductor”.* Advanced Science news (2013)